Vaulted Earthen Floor Systems for Low-Cost Housing Construction

by

Sabrina Gaitan

B.S. Civil Engineering
University of Notre Dame, College of Engineering, 2020

Submitted to the Department of Civil and Environmental Engineering in partial fulfillment of the requirements for the degree of

MASTER OF ENGINEERING IN CIVIL AND ENVIRONMENTAL ENGINEERING

at the

MASSACHUSETTS INSTITUTE OF TECHNOLOGY

June 2021

Signature of Author .....
Department of Civil and Environmental
May 14, 2021

Certified by .....
John Ochsendorf
Class of 1942 Professor of Civil and Environmental Engineering and Architecture
Thesis Supervisor

Accepted by .....
Colette L. Heald
Professor of Civil and Environmental Engineering
Chair, Graduate Program Committee

Vaulted Earthen Floor Systems for Low-Cost Housing Construction

by

Sabrina Gaitan

Submitted to the Department of Civil and Environmental Engineering
on May 14,2021 in partial fulfillment of the requirements for the
Degree of Master of Engineering in Civil and Environmental Engineering

Abstract

This thesis explores the viable geometries of earthen vaulted floor systems for low-cost residential construction. Typical structural floor systems consist of a reinforced concrete flat slab, which is problematic as concrete and steel are expensive, carbon-intensive materials. As urbanization rates increase globally, informal and structurally inadequate settlements become more ubiquitous as a result. Vaulted structural floor systems can be constructed from earthen bricks to reduce cost and environmental impact. This thesis aims to investigate equilibrium solutions of barrel-vaulted structures through the use of local earth materials in emerging economies, with a particular focus in Central and South America.

While artisans have been constructing vaults for centuries as roofing systems, this thesis investigates the highly indeterminate structural behavior and design of shell structures to broaden the scope of their application such that they can also serve as floor systems. Through the lower bound principles of masonry structural design, the spanning limits of this structural form are presented for adobe, compressed earth blocks (CEB), and compressed stabilized earthen brick (CSEB). The analysis of unreinforced masonry vaults is further explored in three dimensions through form finding methodologies that implement linear optimization to investigate viable load paths within a defined area under specified boundary conditions. The application of three-dimensional analysis introduces two-way behavior within the vault, decreasing the reaction forces, and ultimately reducing the cost of construction. This thesis shows the range of possible spans using unfired adobe, CEB, and CSEB for vaulted earthen floor systems in the residential sector.

Thesis Supervisor: John Ochsendorf
Title: Class of 1942 Professor of Civil and Environmental Engineering and Architecture

Acknowledgments

First, I would like to thank The National GEM Consortium in conjunction with Kiley Clapper and Scott Tirrell for the financial support to attend MIT, without which this journey would not have been possible.

I am grateful to my advisor, John Ochsendorf, for pushing me to explore the realm of masonry structures and engaging me to understand the mechanisms behind them. Thank you for listening to my interests and helping me tailor my thesis to my passions, and inspiring me to constantly search for better results. Thank you to Professors Caitlin Mueller and Josephine Carstensen for their patience and continued support throughout the year in my academic endeavors. In addition, I thank William Baker, for his assistance in advising the MEng students this year, and for his personal commitment to teaching me the application of airy stress functions. His expertise and enthusiasm gave me a new-found appreciation for the world of structural engineering. I thank Lara Davis for her work at the Auroville Earth Institute and Ramon Aguirre for his work at the *Instituto de Bovedas Mexicanas,* and for engaging in conversations about the constructability and application of vaulted systems. Both Lara and Ramon provided great visualizations of vaults being implemented in India and Mexico.

I would like to thank Carene T. Umubyeyi, for choosing to spend her UROP working with me to conduct research and further my results. Thank you for your relentless hard work and dedication in helping me size beams, and learn more about the history of earthen vaults. To Demi Fang, for her constant assistance and patience in teaching me to learn Grasshopper and trouble shoot technical problems. I sincerely appreciate the time spent on helping push my thesis further and providing me with a multitude of great resources. To Yijiang Huang for his work to produce a force density code used in this thesis. I would like to thank my peers in Course 1 for providing me with a sense of community and friendship despite the year being virtual. To my colleague and longtime friend, Grace Jagoe, for listening to my ideas and giving me productive feedback.

Finally, I would like to thank my family and friends for the constant support and love. To my parents, Clara and Mario Gaitan, thank you for the life sacrifices you have made to make me the person that I am today, and inspiring my aspiration to be of service to others. Lastly, to Kenneth Fitzpatrick, for constantly being a source of encouragement in such a challenging year.

Table of Contents

List of Figures

List of Tables

Chapter 1

1.1: Introduction

This thesis develops two- and three-dimensional equilibrium solutions for shallow masonry vaults to serve as low cost floor systems in emerging economies. Through ongoing conversations with local builders and new applications of structural analysis, the thesis investigates the potential for earthen vaults as floor systems. By adhering to the compression-only behavior of masonry vaults, the thesis aims to minimize the thrust exerted by the masonry system in order to reduce the amount of necessary reinforcement and explore the capabilities of un-fired adobe brick, compressed earthen brick (CEB), as well as compressed stabilized earthen brick (CSEB).

1.2 Motivation

There is a major disconnect between population growth and the provisions of adequate housing in Latin America. Since 1950, the urbanization rate in Latin America has increased by 93% ("Urbanization in Latin America" 2017). This issue in conjunction with the fact that the world's largest migration crisis may now exist in Latin America, has contributed to a housing deficit (Triveno and Nielsen n.d.). Locals in these communities live in low quality houses that lack security. Migrants are being forced to find temporary settlements built from inadequate materials in public areas that tend to lack sanitation and clean water. In Central America, informal settlements serve as housing for 29% of the urban population, and up to 45% in countries such as Guatemala and Nicaragua (Eurosocial 2020).

This problem is not unique to Central America, and the world is rapidly urbanizing, resulting in one billion people living in slums and informal settlement globally (United Nations 2020). As the housing crisis grows, the need for quality, affordable homes become more urgent. In addition to being affordable and safe, the scale of housing needed will require increased consideration for greenhouse gas (GHG) emissions due to building materials. Researchers have identified the influx of barriers that exists in order to improve housing such as poverty, lack of infrastructure, land tenure, and more. This thesis explores the issue of inadequate infrastructure that can be solved through the use of local materials for structural floor systems. The introduction of industrial materials such as concrete and steel have overlooked the use of earthen

materials for construction, a problematic issue in many countries, where steel and cement materials are expensive. Local materials must be used in combination with innovative sustainable designs to enhance the built environment in these communities.

Using earthen vaulted systems as a substitute for flat concrete slabs in floor systems represents a viable solution to this problem. This proposed system can be constructed through two techniques, the Nubian Vault technique and the pitched-brick vault technique which will be discussed further in Chapter 2. Both vault typologies can be constructed with minimal formwork and can be viable for the solutions proposed in this thesis. Organizations across the globe have used both processes as roofing systems to provide affordable housing opportunities, but not many have explored the use of these systems as floors. This thesis investigates the limits that earthen vaults can safely span, in order to significantly reduce the cost of housing for low-rise construction.

1.3: Research Contributions

This thesis explores the engineering viability of using earthen material to build vaults for floor systems. Earthen vaults have been used recently in structures such as the Mapungubwe National Park in South Africa (Figure 1-1), revealing the potential to avoid the environmental and economic costs of conventional solutions (Ramage et al 2010). The Sustainable Urban Dwelling Unit (SUDU) Project, an initiative that began in 2010 in Ethiopia, used rammed earth in conjunction with vaulting techniques to build simple two-story housing complexes that could be easily expanded (Hebel et al 2015). Additionally, the Auroville Earth Institute, a non-profit organization centered in India, has explored the use of earth based technologies to build low cost sustainable dwellings through intensive research. They have explored the construction process of domes, vaults, and arches, in the context of floor and roof systems in a training manual for architects and engineers that is useful in understanding the behavior of masonry systems. The Auroville Earth Institute provides detail on how to analyze the stability and thrust values of masonry arch structures through the equilibrium methods, and how to build these structures (Auroville Earth Institute n.d.). This thesis applies lower bound principles of masonry structural design following Heyman (1995) to explore the viable geometries for earthen vaulted floor systems by analyzing multiples combinations of parameters such as the span and rise of an arch.

The structural analysis presented here is for barrel vaults, and does not consider domes or groin vaults or more complex geometries. The goal is to understand the behavior and structural stability of masonry arches and the realm of geometries that can be safely built to build low-cost, low-carbon housing. This thesis reveals the potential of earthen materials to withstand floor loads while minimizing expensive and carbon intensive materials such as steel and reinforced concrete.

(a)

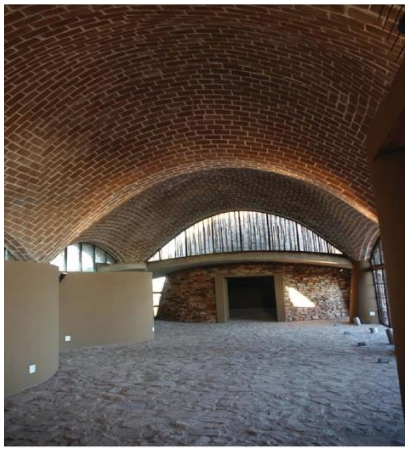

(b)

(c)

Figure 1-1: Mapungubwe National Park in South Africa built from 2008-2009 (a) the interior of the center (b) workers testing the stability of the vault (c) from Ramage et. al (2010)

1.4: Research Objective:

The thesis investigates different parameters of vaulted systems such as the span, rise, and material strength to develop solutions in equilibrium. The following questions are investigated:

- For what combinations of span to height ratios can earthen brick be used while remaining below the safe allowable design stress?
- How do the minimum horizontal thrust values change with different assumptions of boundary conditions and different analysis methods?

- What is the minimum amount of concrete and steel necessary to build a vaulted masonry floor system?

This thesis answers these questions through analysis of the equilibrium state of masonry structures. Unlike typical structures, the failure of masonry arches typically occurs from instability not from the material's lack of material strength capacity (Heyman 1995). However, when using weaker earthen materials, the compressive strength of the earthen brick may limit the safe design of the structure. Conventional linear elastic finite element analysis will not suffice because it will assume that the material can resist tension when it cannot, and thus lead to erroneous results. For this reason, equilibrium of brittle arch structures is best understood through limit analysis that uses compressive thrust lines to gauge stability.

Through these guiding principles as well as computational form finding, this thesis investigates two dimensional and three-dimensional equilibrium solutions of masonry barrel vaults, exploring the range of span to height ratios, referred to as aspect ratios, that can be used for the purpose of creating efficient low-cost vaulted floor systems. Additionally, this thesis serves as a design methodology for organizations and communities interested in creating safe floor systems out of local materials.

Chapter 2 : Literature Review

2.1: History of Masonry Arches

The masonry arch is an integral structural element that has been used for millennia. Archaeologists uncovered one of the first arches through the excavation of ruins in Babylonia, and dated the arch back to 1400 BCE (Newman 2021). Arches were primarily utilized to span large areas that were not possible with traditional building techniques (Beall 2012). These historical structures reinforce the advantages of masonry arches due to their ability to act in pure axial compression ("Brick Masonry Arches" 1995). In 1675, Robert Hooke formalized the structural action of an arch in an anagram that defined the relationship between a hanging chain that behaves in pure tension under self-weight and the inverted arch that behaves in pure compression. Hooke's theorem states that, "the funicular shape that a string or chain takes under a set of loads, if rigidified and inverted, is an ideal shape for an arched structure to support the same set of loads" (Heyman 1995). Hooke's principle is the foundation for understanding masonry arches and has been used to design and assess a multitude of structures.

2.2: Masonry Mechanisms

For many structures there are three main factors that are important in structural analysis: strength, stiffness, and stability (Heyman 1995). In masonry, however, stability is the most critical aspect, as most masonry structures fail as a result of instability rather than limited material strength. Heyman (1995) introduced the following three critical assumptions of masonry for the limit analysis of masonry structures:

1. Masonry has no tensile strength
2. Masonry has infinite compressive strength
3. Sliding does not occur between masonry units.

The compressive strength of most masonry vaults is significantly higher than the stresses the vault will ever experience due to loading, and the tensile capacity of masonry is near zero. Given this unconventional behavior, typical linear elastic finite element analyses cannot be used as it does not say anything about the stability of the masonry system. The nature of a masonry structure can be visualized through thrust lines: "a theoretical line that represents the path of the resultants of the compressive forces through the structure" (Allen et al 2012). A thrust line has a

vertical component from the self-weight and applied gravity loading, and a horizontal component known as the horizontal thrust. A compressive line of thrust due to the applied loading can be found through any number of equilibrium techniques, such as graphic statics (Figure 2-1). If the line of thrust is contained everywhere within the masonry, then the arch is in compressive equilibrium with the applied loads. Most masonry arches are statically indeterminate and can contain a range of horizontal thrust values within the thickness of the arch.

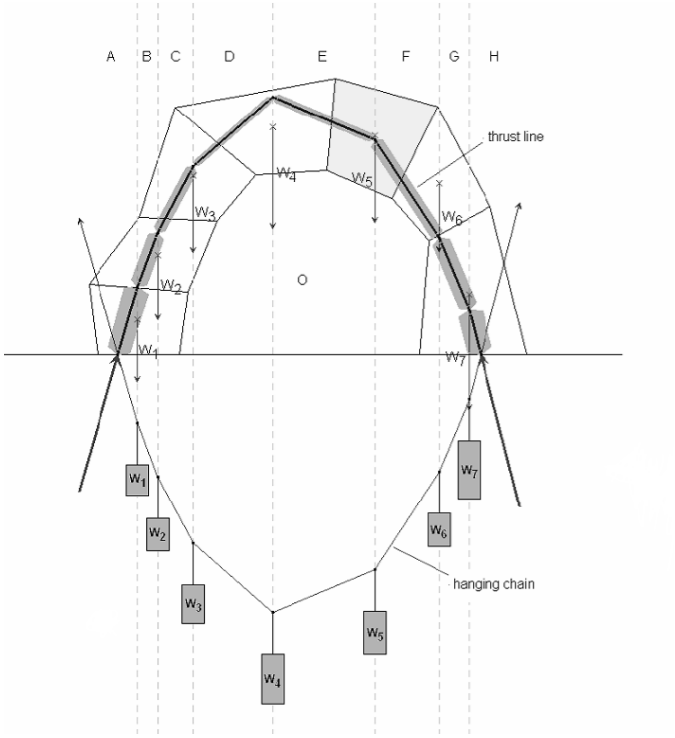

Figure 2-1: A stone arch and one possible thrust line and corresponding hanging chain, after Block et al. (2006).

Heyman (1995) analyzes the behavior of unreinforced masonry through the theory of limit analysis and discusses how the shape of the thrust line within masonry is highly sensitive to small changes in the position of boundary conditions. Moving the abutments of a rigid-block arch by any increment will produce a new equilibrium state of the structure, one of an infinite number of potential states. Thus, the safety of the structure becomes almost fully dependent on geometry. Yielding of the abutments is inevitable. In response as the thrust line changes the arch may form cracks in between points of contact of the rigid block components. Figure 2-2 (a-b) depicts this behavior, as the structure forms cracks, which can be idealized as hinges, when the thrust line touches the outer and inner limits of the arch at the extrados of the crown and at the

intrados of the abutments. These hinges make the masonry arch statically determinate. Through equilibrium equations, the internal forces can be solved for a variety of possible hinge locations.

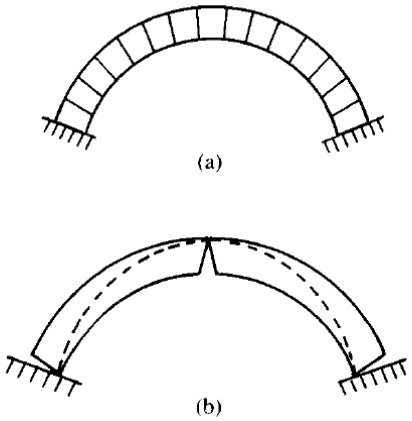

Figure 2-2: Hinging of a stable masonry arch on spreading supports, after Heyman (1995)

A stable arch has three hinges, but the formation of a fourth hinge due to increased or asymmetrical load will lead to the collapse of the structure. This phenomenon can be seen in Figure 2-3, as load P increases enough to cause the formation of four hinges (the black dots), resulting in collapse. The design of masonry structures becomes highly dependent on geometry and on preventing the formation of sufficient hinges to create a collapse mechanism. As long as the line of thrust remains within the masonry, the structure will remain in full compression and be stable.

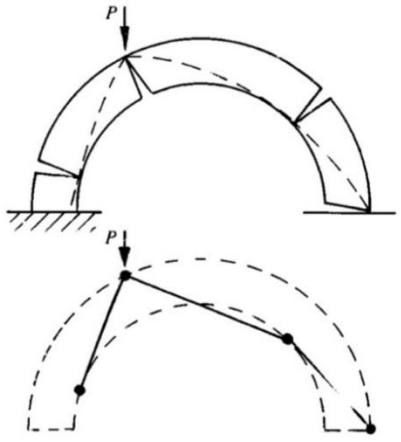

Figure 2-3: Collapse mechanism of an arch, after Heyman 1995

Based on the Safe Theorem which states: "if it is possible to find an internal system of forces in equilibrium with the loads which does not violate certain material assumptions, the structure will not collapse, it is "safe" (Heyman, 1995). There is an infinite range of possible lines of thrust within an arch lying within the maximum and minimum bounds. The thrust line will change as the abutments inevitably move, but the path of compressive forces will remain within the boundaries of the arch, maintaining equilibrium, and not forming more than three hinges. While the exact position of the thrust line is unknown, a safe structure can still be designed through this theorem, provided that the stress capacity of the masonry is not exceeded. For most brick and stone arches, the compressive stresses are relatively low, even in the hinge location, but for weaker earthen arches, the compressive stresses will limit the safe span of the arch.

Block et al. (2006) depicts this discrepancy through the analysis of two simple arches under self-weight. In Figure 2-4, there are two arches, (a) and (c), that represent semi-circular masonry arches with thickness to centerline radius ratios of .08 and .16, respectively. The finite element analysis depicts internal stresses for both arches on the left side, and suggests that there is no great difference between their structural behavior. However, the right-hand side represents the compressive thrust lines created through limit analysis, where it is clear that arch (a) is not thick enough to contain the thrust line and would thus fail under its own self-weight. Finite element analysis does not represent this failure clearly, thus requiring methods such as limit analysis to evaluate equilibrium of masonry arches.

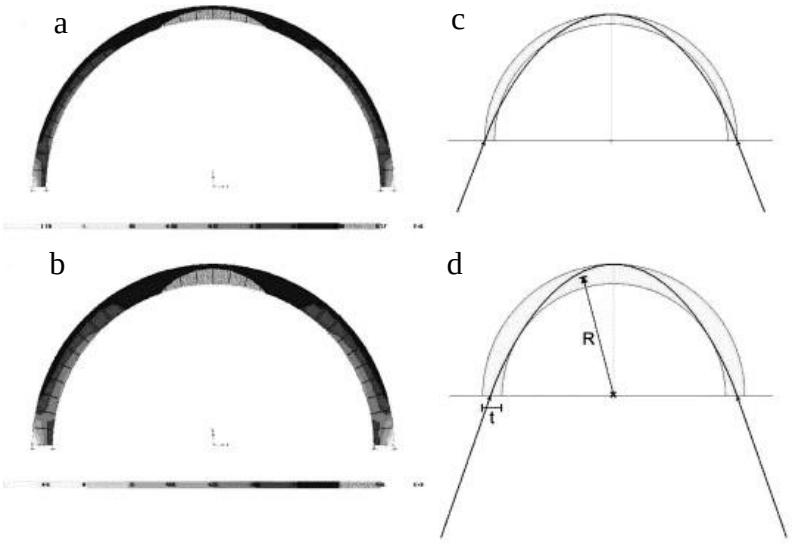

Figure 2-4: Arches (a) and (b) analyzed through finite element analysis, arches (c) and (d) analyzed through limit analysis using compressive lines of thrust after Block et al. (2006)

2.3: Form Finding of Compression only Structures

Compression only structures can achieve an efficient structural form by placing material along the line of thrust in compression. As stated by Veenendaal and Block (2012), the idea that form follows force is predominantly applicable to structures that behave purely axially. With bending not being a concern, the shape is easily determined by the forces that the structure must withstand. Optimal solutions for different sets of geometries depending on the loads applied to the system can be found through form finding. Compression-only shells were form-found by Frei Otto and Heinz Isler through physical models, but this was time consuming and rather costly (Block et al 2011). Experts have introduced different numerical form finding methods such as the force density method, dynamic relaxation, and thrust network analysis (Block et al 2012). In addition to equilibrium calculations for two- and three-dimensional equilibrium, this thesis explores the use of the force density method to determine possible minimal thrust states for masonry vaults.

Form finding is defined as "finding an optimal shape of a form-active structure that is in a state of static equilibrium" (Veenendaal et al 2012). Form finding can be interpreted in a variety of different contexts, but this thesis refers to specifying the conditions of a structure and finding the form that meets those conditions. While form finding can be divided into categories, the

force density method falls into the geometric stiffness family, as it is independent of material properties (Schek, 1974; Veenendaal et al/ 2012).

The force density refers to the force-length ratio for every member of the structure. Each member in the structure is given a single force density value. This parameterization allows for one equilibrium solution to be found through linearization. By altering the force density values, an abundance of different equilibrium shapes can be made. It should be noted that additional constraints can be added so that the force densities are not freely chosen, making the force density method non-linear (Schek 1974). As mentioned previously, an advantage of using the force densities of a structure is that they do not rely on the type of material of the structure, taking out material constraints on the equilibrium solution of the shape. This allows for any material to be chosen without changing the configuration of the structure (Linkwitz, 2014).

This method was used to solve for the equilibrium position of flexible networks through a linearization process with a single solve, meaning that the method is not an iterative process like other types of form finding. Since shell structures are highly indeterminate, the equilibrium solution will change given different sets of loading scenarios. By assigning force densities to the members of these structures, a unique equilibrium solution can be found for a given loading.

In antiquity, the idea of stress values does not exist, creating a geometrical factor of safety that did not consider the strength of the structure but rather the shape of it. As stated by Dahmen and Ochsendorf (2012) in a book chapter on designing earthen arches, the designer must find a suitable geometrical form for which the structure remains in compression under any loading scenario.

2.4: Vaulting Techniques for Floor Systems

The practice of constructing vaults out of earthen material can be traced back to at least 1230 BCE at the Ramesseum at Luxor (El-Derby et al. 2016), built according to the Nubian vault technique. The largest span achieved is the 24m (80 feet) span in earthen brick in 540 AD at the Taq-I Kisra arch in modern-day Iraq. These arches are particularly noteworthy because they were built with minimal to no formwork and they have survived largely intact from antiquity until the present day.

Earthen masonry, in contrast to Portland cement-based concrete, has a low environmental impact, as it does not release as much carbon dioxide into the atmosphere. While earthen bricks

do not have the same magnitude of compressive strength as concrete, they can still be used to develop safe structures when used correctly. This thesis investigates the use of earthen material to build shallow brick vaults with minimal form work. The masonry vaults proposed here can be constructed through either the Nubian Vault or the pitched-brick vault technique. The difference between the two construction processes can be seen below in Figure 2-5, with the left side representing the Nubian Vault technique and the right side depicting the pitched-brick vault, which is also known as "bovedas" in Mexico and "de rosca" in Spain. Both techniques follow the principle that inclined bricks are held in place by the adhesion of mortar and the curving geometry of the vault.

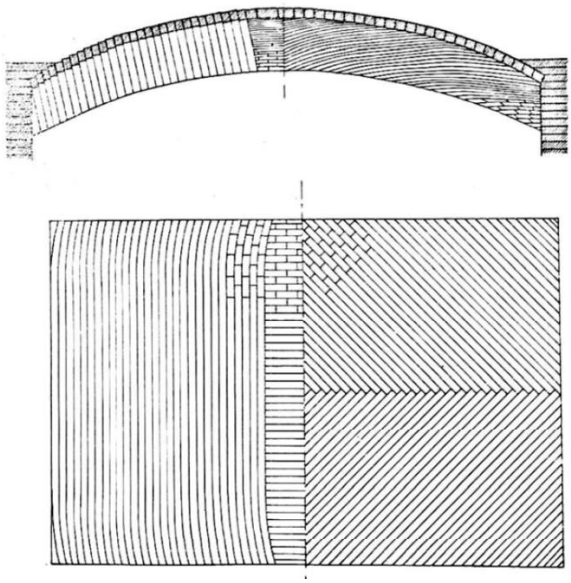

Figure 2-5: The Nubian Vault technique (left) versus the pitched-brick vault technique (right), reproduced in Adiels et al. (2017)

The Nubian vault is a technique dating back to approximately 3500 years ago (Dahmen and Ochsendorf, 2012). This technique was revived beginning in the 1940's by Hassan Fathy (1900-1989), an Egyptian Architect commonly referred to as the "Architect of the Poor" (Steele and Fathy 1988). In 1941, Fathy encountered the use of Nubian vernacular architecture in Aswan, Egypt while on a trip with students visiting historic archaeological sites. Propelled by the desire to incorporate local cultural traditions into the built world, Fathy improved the standard of living in many rural communities. Since then, the technique has been implemented in construction by the Auroville Earth Institute and the International Centre for Earth Construction

among others (Auroville Earth Institute n.d.). Photos displaying the construction process of a Nubian Vault under the supervision of Hassan Fathy can be seen below in Figure 2-6.

1. Shaping the curve into the adobe wall

2. Adjusting the Curve

3. Starting the Vault

4. Starting the Inclined Course

5. First Course

6. Second Course

7. Applying some mortar

8. Third Course

9. Fourth Course

10.The first arch is completed

11. Building arch after arch

Figure 2-6: Nubian Vault Construction, from Auroville Earth Institute (n.d.)

Originally, the Nubian vault works by having the bricks laid leaning, with the first set of bricks typically resting on a wall, as seen in Figure 2-6. The vault is then constructed one arch at a time, with each layer leaning on the preceding arch. The blocks are held together by a binder, such as mud mortar, with the incline of the brick increasing the adhesion between components due to the force of gravity. The Auroville Earth Institute has found great advantage in using compressed stabilized earth blocks because they can be produced with a thickness tolerance of 0.5mm allowing for the mortar joint to be thin. As a result, "the courses can be absolutely vertical as it is not needed any more to incline the courses for the adhesion" (Auroville Earth Institute n.d.).

The pitched brick vault is a related technique from the late third millennium BCE (Oates 1990). It consists of laying bricks consistently with their edges along the long axis of the vault. The bricks are laid from the four corners simultaneously, and each layer is inclined at an angle to rest on the previous layer. When the layering from the four corners converge in the middle, there is a gap that will be filled with brick that is typically of smaller size. A plan section of just the pitched brick vault technique can be seen below in Figure 2-7.

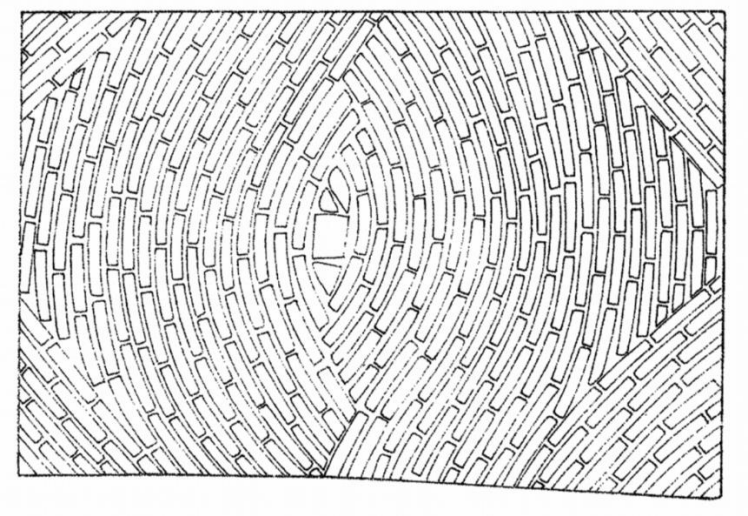

Figure 2-7: Plan View of pitched-brick vault technique, from Oates 1990

2.5 Structural Capacity of Various Earth Materials

Using earthen material to construct arches, vaults and domes has been used for centuries, and have proven to withstand the test of time, with structural longevities of over 1000 years old (Dahmen and Ochsendorf 2012). Adobe was the first material that humans used to build, dating back thousands of years to the earliest human settlements. Compressed earth blocks first started being used in the beginning of the 19th century in Europe, when Francois Cointereaux used hand rammers to compress soil into moulds (Auroville Earth Institute n.d.). Since then, many countries have adapted the use of machines to press soil into regular sized blocks that are denser and stronger than adobe (Auroville Earth Institute n.d.). A major benefit to using earthen material over other options such as concrete, steel, or wood is the minimal environmental impact as earth is low in embodied energy. The strength capabilities of earthen masonry are lower than that of concrete, but when designed carefully and correctly, earthen arches, vaults, and domes serve as sustainable and efficient structural systems (Dahmen and Ochsendorf 2012).

This thesis explores the use of unfired adobe, CEB, and CSEB as potential materials to build earthen vaults. Unfired adobe brick has an ultimate compressive strength that can range from 0.5 to 3.2 MPa. According to the International Building Code 2015, adobe should be designed to have an allowable stress of 45 psi which is approximately 0.3 MPa. This study analyzes a brick of 0.9 MPa ultimate compressive strength, which corresponds to an allowable stress of 0.3 MPa. One can achieve more strength capabilities by using compressed earthen

brick, which has a lower bound ultimate compressive strength of approximately 2 MPa (ASCE 2011). CSEB is formed from CEB stabilized with cement or lime, giving the material an ultimate compressive strength that can range from 7 MPa to 3 MPa depending on the class of soil used (Auroville Earth Institute, n.d.). According to Section 1714 of the International Code Council (2009a), a factor of safety of 2.5 should be used for CEB and CSEB resulting in allowable stress values of 0.8 MPa and 1.2 MPa respectively. In the construction of the Mapungubwe National Park Interpretive Centre, South Africa, engineers designed the shells to have allowable stress of approximately 1.5 MPa, or 30% of the 5 MPa ultimate stress (Ramage et al. 2009). The Auroville Earth Institute recommends the use of CSEB for vault construction, as it can be produced with a thickness tolerance of 0.5 mm, whereas adobe typically cannot be produced as regularly. In addition to this, CSEB has an embodied energy that is 10.7 times less than country fired brick and a carbon emission that is 12.5 times less. The spanning capabilities of CSEB and its differentiation from adobe and CEB will be explored further in Chapter 3.

2.6 Vaulted Floor Systems to Save Weight and material

The self-weight of floor systems can consist of up to 50% of the load when constructing a building. Floor structures commonly behave in bending, resulting in copious amounts of materials that has sufficient tensile and compressive strength. This is problematic, as the built industry is facing more and more pressure to reduce carbon dioxide emissions. Arches and vaults can serve as a more efficient solution to this problem, as their shell structure behaves in compression only, reducing the amount of necessary material for construction. In comparison to typical reinforced concrete slabs, arched floor systems can reduce the total mass by up to 70% (Barentin et al 2020). The Block Research Group at ETH Zurich has developed a funicular floor that utilizes the behavior of arches to reduce the structural volume through strategic placement of material only where necessary to initiate compressive stresses rather than flexural stresses (Barentin et al 2020). With these findings in mind, this thesis will further explore the limits that compression only structures can span for structural floor systems.

2.7: Projects Using Vaulted Structures in Emerging Economies

The Auroville Earth Institute (AEI) in India, has been building with arches, vaults, and domes, for more than three decades now (Auroville Earth Institute n.d.). The organization makes

use of compressed stabilized earthen blocks (CSEB) as it has both dry and wet strength values, and is produced with a thickness tolerance of .5mm, whereas adobe only has dry strength and cannot be produced with such regularity. In addition to this, the AEI uses the Nubian vault technique as well as the free spanning technique. This is a variation of the Nubian Vault technique which lays the horizontal course (via corbelling) until the limit of stability is reached and the vertical courses are used (Auroville Earth Institute n.d).

Similarly, in Mexico there is an organization called *Instituto de Bovedas Mexicanas* led by Ramon Aguirre that implements this ancestral technique of pitched-brick vault in contemporary life, as seen in Figure 2-8 (IBOMEX 2019). The *Instituto de Bovedas Mexicans* has used this technique in building roof structures with relatively deep rises. The rise of the arch is approximately 30% of the span because it is the most common way to build structures without the use of formwork, and with this inclination the brick pieces (5x10x20 cm) are very easy to hold (Aguirre 2021). However, this group has not comprehensively explored the potential for vaults to construct contemporary floor systems.

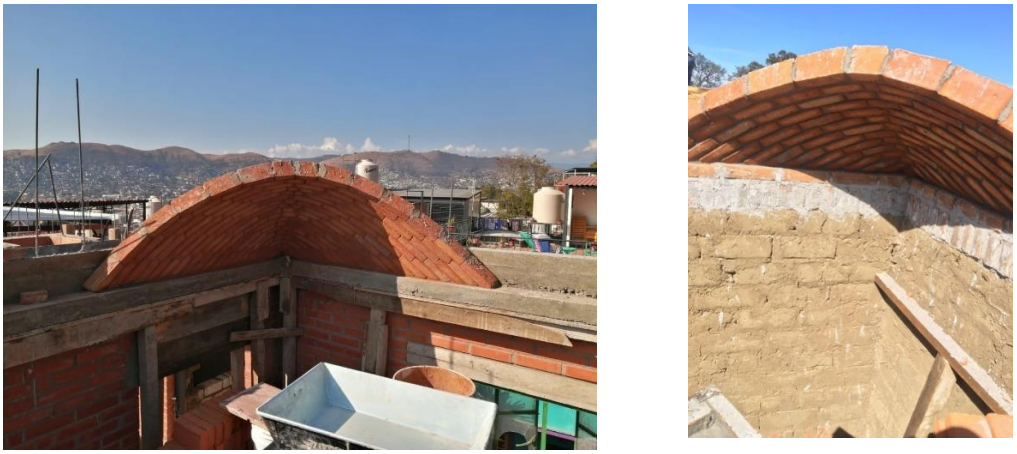

Figure 2-8: Pitched-brick vault construction, courtesy of Ramon Aguirre

Aside from this work done in Mexico, there is a French non-profit organization called *Association La Voute Nubienne* (AVN) that is focused on building sustainable houses in West Africa by training local builders on using the Nubian Vault technique for roof systems, using adobe brick (La Voute Nubienne n.d.). Since deforestation has led to a scarcity of timber in countries such as Mali, Senegal, and Ghana, it is important to learn how to build infrastructure

without the use of formwork. AVN has found the vaults to be not only affordable and sustainable but also comfortable in terms of thermal and noise insulation (The Nubian Vault Concept, n.d.).

In addition, the Adobe Alliance in the United States is a nonprofit that is concentrated on training communities to build vaults and domes with adobe for inexpensive roofing purposes. This organization recognizes the steep cost of buying industrial materials as well as the wood and tools needed to build traditional roofing systems. The Adobe Alliance has taught a multitude of self-reliant families in Texas to build mud brick roofs that don't require the use of wood, significantly reducing costs (The Adobe Alliance, 2020).

The SUDU project in Ethiopia created sustainable homes out of local materials, deviating from traditional building methods and gravitating towards vernacular technologies. The dwelling units required minimal formwork and used materials that had a low carbon footprint. Through the use of rammed earth, the project implemented tile vaulting on the first ceiling and the same technique on the roof but with bigger loam bricks. The second floor of the project was constructed with pressed loam stones and required minimal formwork (Hebel 2015). The Mapungubwe National Park Interpretive Centre implemented soil cement tiles to build three vault types, one of them being a shallow barrel vault to support a floor, similar to the system proposed in this thesis (Ramage et al 2010), but in earthen tile vaulting, rather than pitched brick vaulting.

Both Wilson (2016) and Jagoe (2021) conduct research on the behavior and application of masonry to propose the construction of a vaulted earthen floor system and an autoclaved aerated concrete (AAC) tile vaulted floor system, respectively. Wilson (2016) explores flat masonry domes as a low cost flooring system in the housing sector of India. Similar to Wilson's research, this thesis proposes the use of unreinforced vaults as floor systems where no steel is utilized inside the vault or fill. Wilson (2016), however, proposes the use of a shallow earthen dome rather than a barrel vault. Jagoe (2021) explores the application of masonry construction through the use of AAC tiles and fast-setting mortar to produce a vaulted floor with a 67% reduction in structural weight to that of a conventional concrete flat slab. The research completed by both Wilson (2016) and Jagoe (2021) use equilibrium methods and plastic theory to ensure the strength and stability of masonry vaulted floor systems.

All of these organizations, projects, and works are actively promoting the use of earth vault systems to provide a sustainable solution for affordable housing. While the Auroville Earth

Institute has analyzed earthen vaults in the context of floors, the *Instituto de Bovedas Mexicanas*, *Association La Voute Nubienne*, and Adobe Alliance have only used earthen vaults in the context of roof systems. The SUDU Project and the Mapungubwe National Park have implemented the use of vaulted floor systems. Although these projects set a precedent for vaults made of earthen material, the full potential of these vaults has not yet been maximized in the housing sector. This thesis aims to further explore the capabilities of earthen materials to withstand the demand of floor loading, and reveal the extent to which local materials can serve as a replacement to traditional reinforced concrete flat slabs for stable floor systems. While the exact load paths of forces are only known to the vault itself, the load capacity of earthen vaults can be quantified through structural analysis.

2.8 Chapter Summary

Vaulted earthen systems have proven to be economically and environmentally sustainable solutions to the housing crisis that exists globally. However, there is limited literature that provides guidelines for calculating the safe design of earthen brick vaults for floor systems. There are currently no examples of publicly available calculations that local builders can replicate for the implementation of these structures. The Mapungubwe Interpretive Center built a shallow barrel vault, but there is no published description or details of this floor system. While the strength of earthen brick has been a large topic of research, it has been mainly concentrated towards its ability to serve as walls bearing vertical loads. This thesis will thus explore the structural possibilities for spanning with earthen material.

Chapter 3 : Two-Dimensional Structural Design

A primary objective of this thesis is to determine the maximum distance that can be safely spanned using adobe, CEB, or CSEB. The investigation begins with a two-dimensional analysis for a range of geometrical and material parameters and specified boundary conditions for the system seen in Figure 3-1. The proposed vault consists of a parabolic brick arch, a fill that can have variable density, and a brick slab on top. It is supported continuously on two parallel edge beams. For the shallow arches considered in this thesis, the loading due to self-weight as well as a uniform live load is considered for a parabolic arch, as explored Wilson (2016). A reinforced concrete ring beam is cast to support the brick vault. The ring beam must be designed to contain enough steel to resist the outward horizontal thrust at the base of the vault. Depending on the boundary conditions, the ring beam may also need to have not only tensile capacity but also flexural capacity. For example, the Auroville Earth Institute design manual constructs vaulted earthen floor systems that rest on walls, and as a result the only steel needed to support the system are tension ties, and flexure is not considered (Davis et al. 2020).

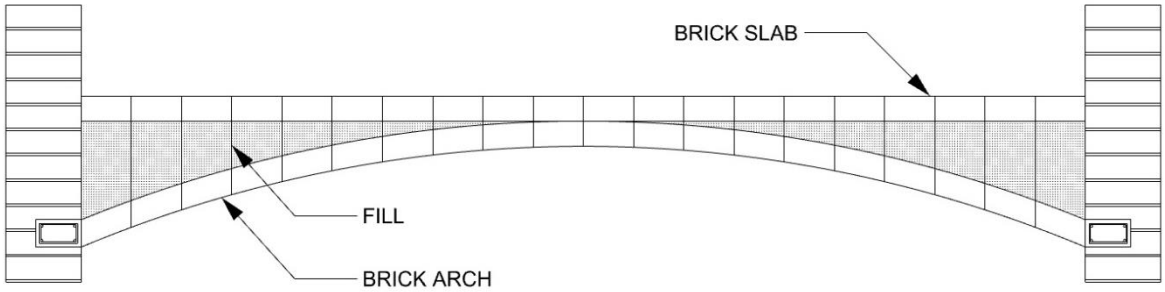

Figure 3-1: Proposed vault system for a parabolic arch

3.1: Two-Dimensional Structural Analysis of Earthen Arches Supporting a Floor

The following geometrical and materials parameters describe the calculations done in this chapter:

- Dimension (L): the span of the vault, in meters
- Rise (D): the height of the arch measured from the crown to the base, in meters
- Brick Thickness (T_b): thickness of the earthen arch, in meters
- Slab Thickness (T_s): thickness of the slab on top of the fill, in meters

In the proposed vault it is assumed that the force only travels within the thickness of the brick. The analysis begins by analyzing half of an arch split up into ten equal segments, assuming a one-meter wide strip into the page, as seen in Figure 3-2. The centroid of each segment is found, and the dead load due to the fill of that segment, as well as the dead load due to the weight of the brick and slab is placed at this point. The density of the fill is estimated to be 2400 kg/m^3, inspired by the 150 pcf assumption done by the Indian Standard code for the construction of floors using curved shell units (IS 632 1984). For this thesis, two fill scenarios are investigated; the 2400 kg/m^3 density as well as 42% of this value. The density of the brick and slab is approximated to be 1900 kg/m^3 each, similar to the density of brick used by the Auroville Earth Institute (Davis 2021). Additionally, a uniform live load of 1900 N/m^2 is applied to the system, in accordance with common building codes for residential floor systems [ASCE/SEI 7-10]. The resultant force due to the live loads behaves at *L/4*.

The crown has no fill above it, and as one moves away from the crown the fill increases, by splitting the half arch into ten segments, this methodology considers the change in load along the vault. The minimum thrust value is obtained by taking the sum of the moments about Point C, assuming that the thrust values act at the top face of the brick (Figure 3-2).

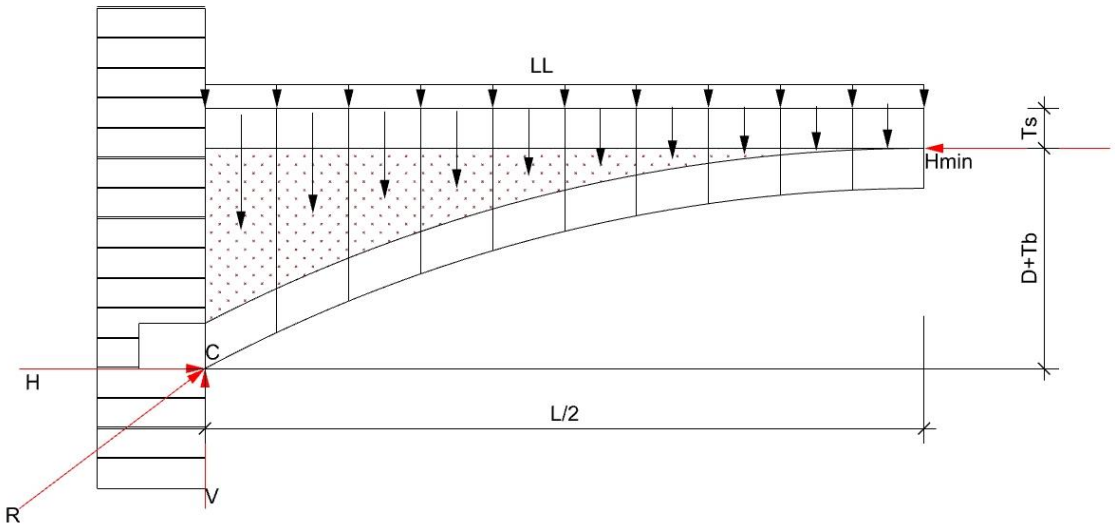

Figure 3-2: Assumed equilibrium state for computing minimum horizontal thrust, H_{min}, in a 2D earthen arch where D is the rise at midspan and T_b is the brick thickness

The minimum thrust value is obtained from a lower bound solution. Although this solution gives a minimum thrust to the system, it is not a realistic solution because it does not

account for a stress distribution on the material. A rectangular stress block is assumed to behave on the entire face of the brick arch, as seen in Figure 3-3. The forces no longer act at the top of the brick, but now at the middle of the brick thickness. The moments were taken again about point *C*, to obtain a horizontal thrust value that is used to calculate the necessary amount of steel needed to support the system. The horizontal force calculated from the stress block assumption was approximately 10% greater than the minimum horizontal force.

The arch displayed in Figure 3-3 only represents a one-meter wide strip. By extruding the system by the proposed width, tension steel can be sized to resist the horizontal thrust exerted by the entire barrel vault. An in-depth example calculation can be seen in Appendix A. This procedure is replicable for a variety of spans and material properties.

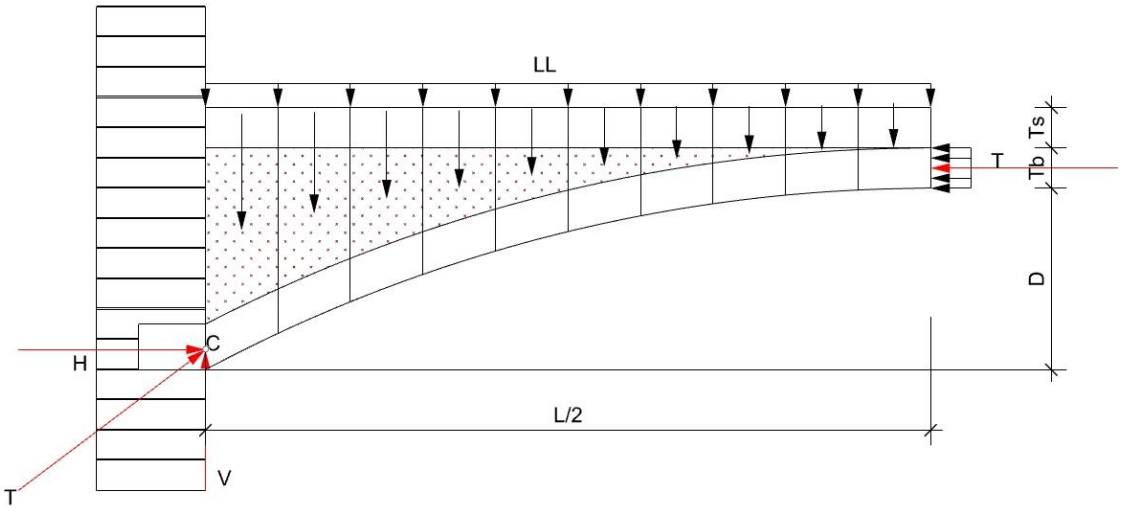

Figure 3-3: Stress block assumption for horizontal thrust calculation in an earthen barrel vault supporting a floor system

3.2: Lighter Fill Density Consideration

The above calculations for the stress block configuration are performed for a variety of vault geometries with span to rise ratios of five, ten, and twenty. For these geometries and given loadings, the maximum stress at the support is computed and is compared to the strength of weak adobe brick, compressed earthen brick (CEB), and compressed stabilized earthen brick (CSEB). In addition, two different fill densities are considered. A more conservative fill value resembling the weight of concrete is analyzed in addition to a lighter weight fill.

Reducing the density of the fill could be accomplished in a number of ways, for example by introducing voids into the fill through the use of recycled glass bottles. Within the fill, empty glass beverage bottles can be placed in a staggered arrangement, adding soil between empty spaces along each course. This new vaulted system can be seen below in Figure 3-4, as produced by Carene T. Umubyeyi. Appendix B displays calculations, also produced by Carene T. Umubyeyi, that estimate the reduced fill density by analyzing a 25 by 25 cm square area with a one-meter depth.

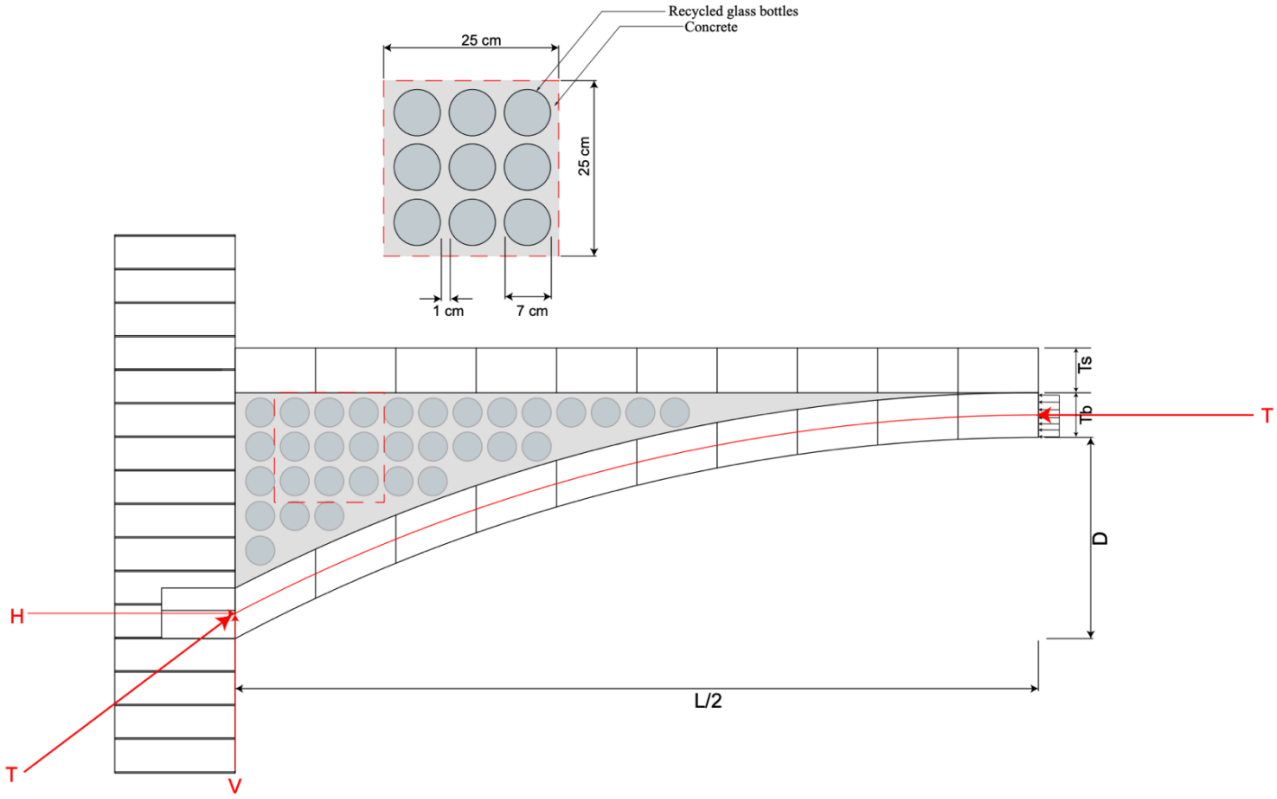

Figure 3-4:Reducing fill density by 44% using recycled glass coke bottles (Image by Carene T. Umubyeyi)

3.3: Two Dimensional Results

3.3.1: Fill Density Scenario 1

The following calculations are performed with a fill density of 2400 kg/m^3. As discussed in §2.5, earthen material has a range of strength values that are dependent on the region and specific mix design. For this thesis, an ultimate compressive strength value of 900 KPa is

assumed for weak unfired adobe, and 2 MPa for CEB, and 3MPa for CSEB. An allowable stress value of 300 KPa, 800 KPa, and 1200 KPa is assumed for the materials, respectively.

Based on these parameters, in conjunction with the calculations described in §3.1, Figure 3.5(a) presents the potential to span different lengths with all three arching materials, i.e. adobe, CEB or CSEB, for different aspect ratios. The aspect ratio is defined as the span length divided by the rise. An aspect ratio of five represents a deeper arch, and an aspect ratio of 20 represents a shallow arch, Figure 3.5(b).

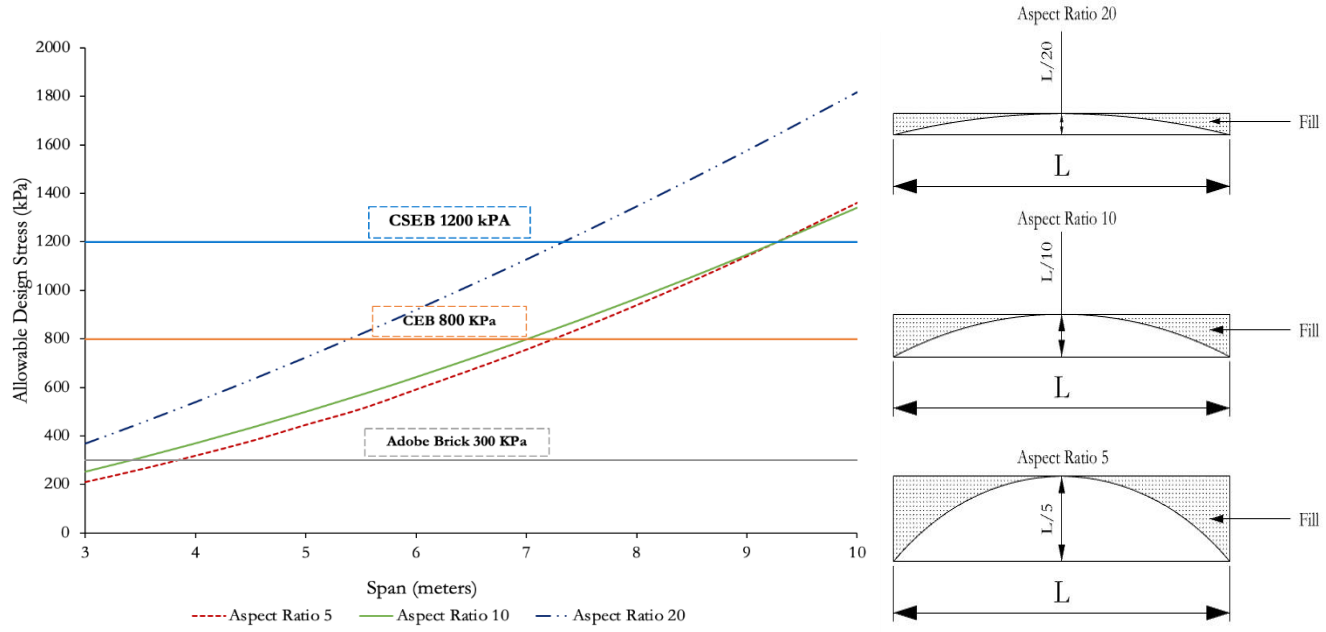

(a) *(b)*

Figure 3-5: Allowable Stress vs. Span Length: Categorized by aspect ratio (Span/Rise) with 2400 kg/m³ fill density (a) Aspect ratio visualization (b)

From Figure 3-5, vaults can safely span up to 4 meters with an aspect ratio of 5, and up to 3.5 meters with an aspect ratio of 10 using weak adobe brick. If builders use CEB with an allowable stress of 800 kPa then one can safely span up to 7 meters with aspect ratios of 5 and 10, and up to 5.5 meters with an aspect ratio of 20. Furthering the strength of material, if builders use CSEB with a strength of 1200 kPa to construct vaults, it is possible to span up to 9 meters for aspect ratios of 5 and 10, and up to 7 meters for an aspect ratio of 20. It is an interesting observation that for this specified fill density of 2400 kg/m³, the stress curves representing the aspect ratio of 5 and 10 begin to merge. While having a deeper arch (aspect ratio 5) results in a

lower thrust value than a shallower arch (aspect ratio 10), the increased fill load after a span of approximately 9 meters counteracts the smaller thrust value resulting in the same stress demand as a shallower arch. The feasible span lengths for each material and aspect ratio are tabulated below in Table 3-1.

Table 3-1: Allowable span lengths considering adobe, CEB, and CSEB for aspect ratios of 5, 10, and 20 with a fill density of 2400 kg/m^3

	Adobe	CEB	CSEB
Aspect Ratio 5	3.75m	7.25m	9.25m
Aspect Ratio 10	3.5m	7m	9.25m
Aspect Ratio 20	---	5.5m	7.5m

3.3.2: Reduced Fill Density

The above results reflect the impact of using a conservatively heavy fill, resembling the weight of concrete. By analyzing the vaulted system proposed in Figure 3-4, with a reduced fill density of approximately 1400 kg/m^3, or approximately 42% lower, new results are tabulated, as displayed in Figure 3-6.

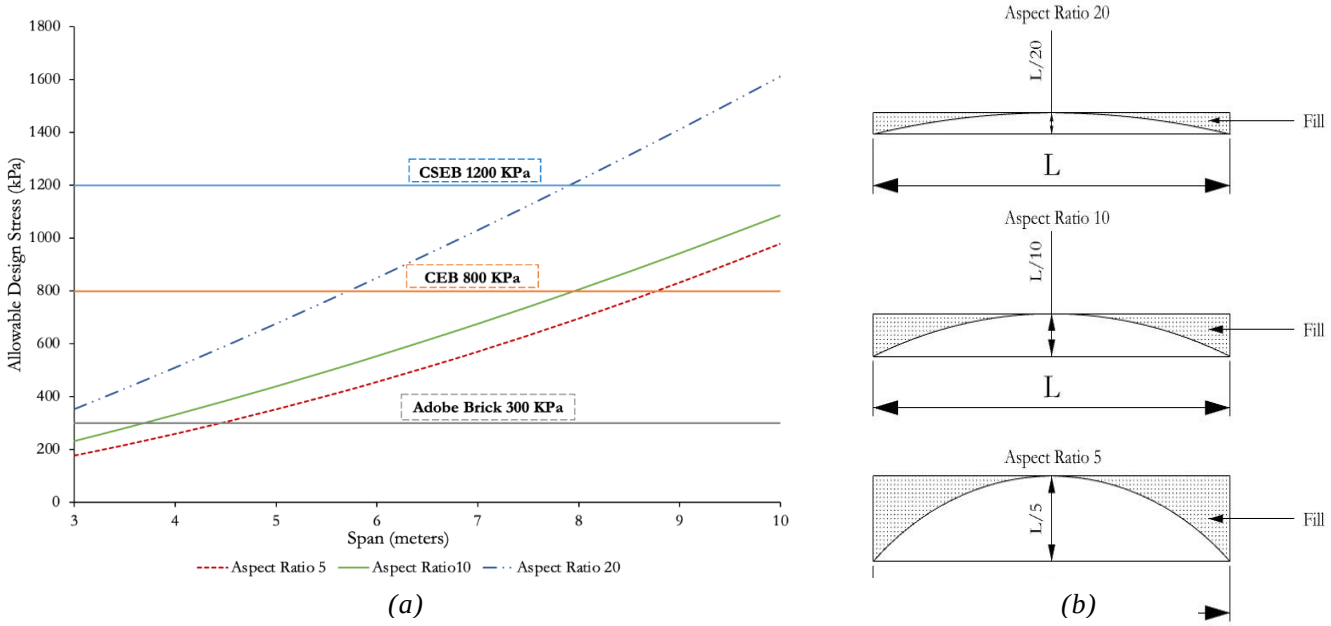

Figure 3-6: Allowable Stress vs. Span Length: Categorized by aspect ratio (Span/Rise) with 1400 kg/m^3 fill density (a) Aspect ratio visualization (b)

The lighter weight fill reduces the dead load in the system and extends the spanning potential for each of the three brick earthen materials considered. With the reduced fill density, builders could span up to 4.5 meters with an aspect ratio of 5, and up to 3.8 meters with an aspect ratio of 10 with weak adobe brick. Through the use of CEB, builders can span up to 9 meters with an aspect ratio of 5, 8 meters with an aspect ratio of 10, and 5.5 meters with an aspect ratio of 5. Furthering the strength of the material through the use of CSEB, builders can span up to 9 meters with aspect ratios of 5 and 10, and up to 8 meters with an aspect ratio of 20. With a lighter fill, the stress curves of aspect ratio 5 and 10 do not intersect, as seen in Figure 3-5. Using a lighter fill allows builders to reduce horizontal thrust by having a deeper arch, as the vertical load caused by the fill has less of an effect on the system. The feasible span lengths for each material and aspect ratio is tabulated below in Table 3-2.

Table 3-2: Allowable span lengths considering adobe, CEB, and CSEB for aspect ratios of 5, 10, and 20 with a fill density of 1400 kg/m^3

	Adobe	CEB	CSEB
Aspect Ratio 5	4.5m	8.75m	10m
Aspect Ratio 10	3.75m	8m	10m
Aspect Ratio 20	---	5.75m	8m

Based on Figures 3-5 and 3-6 the thesis recommends a barrel vaulted system with a span of 6 meters and aspect ratio of 10 using CSEB and a reduced fill density of 1400 kg/m^3. The span of 6 meters and aspect ratio of 10 is recommended as the stress demand of this geometry is well below the ultimate compressive strength of CEB and CSEB, and the geometry covers a suitable distance for most housing needs. CSEB is chosen as it has the best strength capabilities of all three arching materials and can be produced regularly with a thickness tolerance of 0.5 mm (Auroville Earth Institute n.d.). The lighter fill is suggested as it increases the range of spans possible with adobe, CEB, and CSEB. With the lighter fill, the vertical dead load does not affect the allowable design stress, as all aspect ratios have clearly defined trajectories that do no intersect, unlike the results displayed in Figure 3-5. This chapter provides design guidelines for an earthen vaulted floor system considering 2D action. Chapter 4 aims to analyze the same system but in 3D to evaluate the change in total thrust considering two-way action.

3.4: *Chapter Summary*

This chapter demonstrates that earthen brick has sufficient strength to behave as floor systems, and quantifies the spans that are viable using arches and earth material. The required brick strength depends on the arch geometry (i.e. the aspect ratio) and this chapter presents the possible design scenarios for an earthen vault, including consideration of a reduced fill density. Figures 3-5 and 3-6 represent the viable geometries for which different materials can carry loads in compression through an earth masonry barrel vault. A ring beam is necessary in order to resists the tensile thrust at the base that can be resolved through steel reinforcement. The steel quantity requirement for different spans can be found in the design guide in Appendix C for the tensile demand and Appendix D for the flexural demand.

Chapter 4 : Three-Dimensional Structural Design

This chapter analyzes the 3D structural behavior of the proposed vaulted system. It discusses how the horizontal thrust value changes through the analysis of force flow assumptions, a rigid body stress distribution, and computational methodologies, specifically the force density method. The system is assumed to be the same as seen in Figure 3-1, behaving as a barrel vault continuously supported on two parallel edge beams. The only deviation from this boundary condition is for the system proposed in §4.2, which is only supported at the corners of the vault. It is concluded that the thrust of the vaulted system is reduced when analyzed in 3D rather than 2D. This is especially important in the developing world, in which the required steel for the system is governed by the minimum horizontal thrust values to safely support the earthen vaults. The stress values, however, prove to be less clear than analyzing the system in 2D.

4.1: Three-Dimensional Analysis: Two-Way Behavior of Forces

4.1.1: Force Flow Assumptions

The two-dimensional calculations assume that the forces have one-way behavior. However, in reality, 100 percent of the force does not travel directly parallel to the arch span, but rather some percentage of the force travels directly to the corners, provided there is potential for a transverse reaction at each corner. To further investigate this behavior, consider a 4m x 4m plan area, divided into eight 0.5-meter sections, as seen in Figure 4-1.

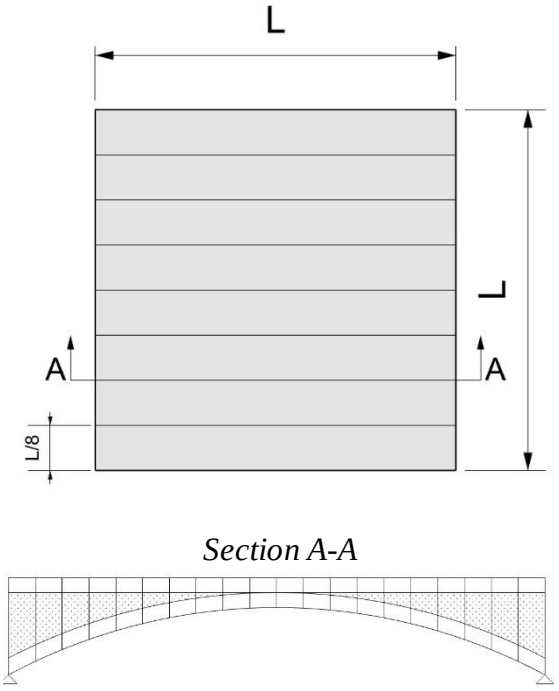

Figure 4-1: Plan view of proposed system (a) elevation view of Section A-A (b)

The total vertical load, V, acting on one strip is taken from the 2D calculations. Then 40 percent of the vertical load is assumed to travel longitudinally along the barrel vault, and the remaining 60 percent of the vertical load is assumed to go directly to the four corners through diagonal arches. This distribution creates a vertical reaction of *0.2V* at edge beam and *.015V* vertical reaction at each corner support, Figure 4-2.

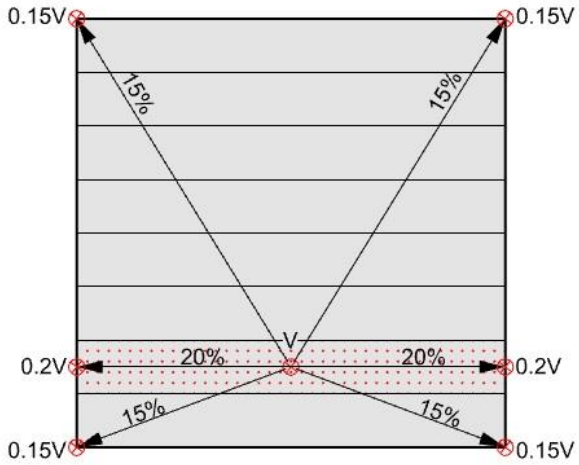

Figure 4-2: Distribution of vertical load

Each individual arch is analyzed considering the percentage of vertical load acting on it. The thrust, *H*, is calculated based on the length and rise of each arch. The live load portion of the load is assumed to behave at the midspan of each arch analyzed. The dead load is divided into ten segments along each arch, proportional to the depth of each segment. The dead load of the system is assumed to behave at each segment centroid, and statics is used to equilibrate the thrust, as done in §3.1. The thrust force obtained from these calculations is then split up into the longitudinal (*T1,T3,T5*) and transverse (*T2,T4*) direction, depending on the angle that the diagonal makes with the corners, as can be seen in Figure 4-3.

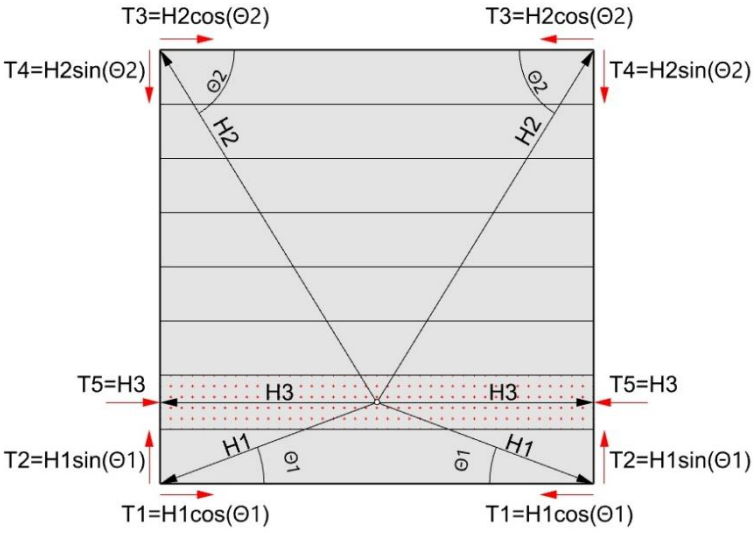

Figure 4-3: Thrust calculations considering diagonals

4.1.2: Thrust Results

For a square vault of 4mx4m, the total longitudinal thrust acting on the system decreases by 4%, which is not significant compared to the original 2D analysis. This system, additionally, decreases the amount of bending the edge beam needs to take as it introduces thrust in the transverse direction, which is not considered in the 2D calculations. These calculations proved to be insightful on the behavior of thrust in the transverse direction, but an even further reduction in thrust, may be possible by exploring other three-dimensional equilibrium calculation methods.

4.2: Three-Dimensional Analysis: Rigid Body

4.2.1: Rigid Body Configuration

To explore the three-dimensional behavior of forces further, a global equilibrium calculation is conducted that considers a quarter of the vault as a rigid body. For the boundary conditions, the rigid body is pinned at the corner and all of the load is assumed to go to this corner, as seen in Figure 4-4.

The rigid body assumption is the state in which all of the forces are balanced in the longitudinal and transverse direction. The "H1" value in Figure 4-4 provides translational equilibrium, while the "H2" value provides rotational equilibrium. Both forces, H1 and H2, are assumed to act at the top of the slab, in order to obtain the minimum thrust values of the system. These thrust results are theoretical lower bound values that are not achievable in practice, and are calculated to give insight to the magnitude of values that are expected

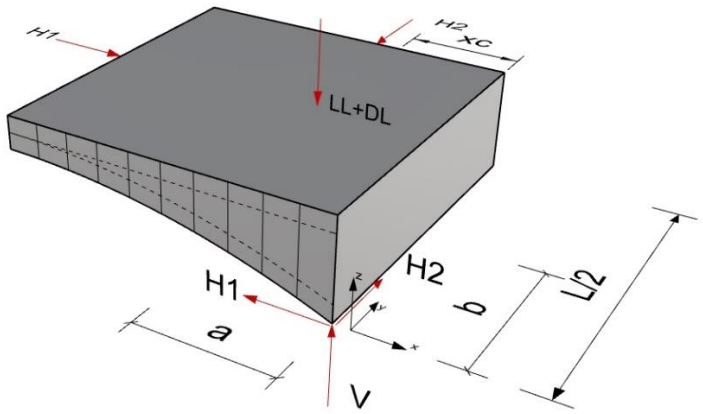

Figure 4-4: Rigid body system for minimum horizontal thrust

The assumed pin connection creates three reactions at the corner point: H1, H2, and V. The total vertical load acting on the vault is taken to be an extrusion of the 2D loads calculated in §3.1, assuming the same brick weight, fill weight, and live load. The centroid of the vault, however, does not coincide with the location of the live load. By taking the sum of the moments of both the dead and live load in accordance with their respective centroids, a singular centroid is found; a distance "x_c" from the y-axis.

By taking the moments about the y and x-axis, *H1* and *H2* are found. In order to satisfy equilibrium in the z-direction, there is a relationship between the distance *H1* and *H2* offset from the origin, values *b* and *a* respectively; this relationship is defined by equation 1.

$$a = \frac{xc}{L/4} * b \qquad (1)$$

To further refine the above calculations a uniform rectangular stress distribution is assumed to act on the left face of the vault system, Figure 4-5. The face is taken to be L/2 meters wide with a thickness equivalent to the thickness of the brick and slab, as seen in Figure 4-6. The same boundary conditions are assumed as mentioned above.

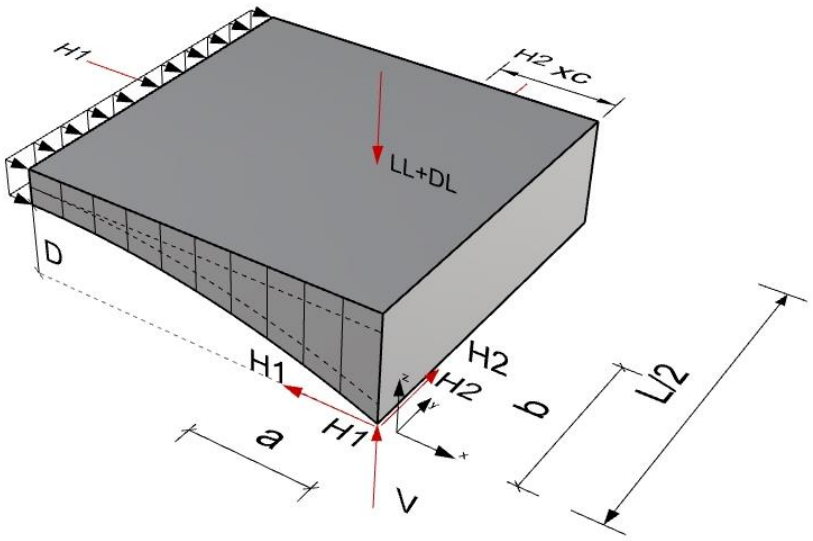

Figure 4-5: Rigid body system stress distribution in equilibrium

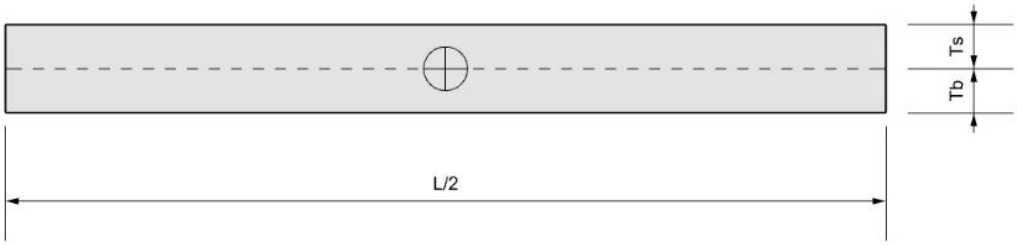

Figure 4-6: Section view of the vault cross-section where horizontal reaction H1 applies uniform stress at the center

With this assumption, the horizontal force, *H1*, acting across the arch direction is found, balancing the moment due to the vertical load. By analyzing the moments about the y-axis, H1 is calculated:

$$H1 = \frac{(LL + DL)(xc)}{(D + .5(Tb + Ts))} \qquad (2)$$

where the variables LL and DL represent the total live and dead load for a quarter of the vault, measured in kN.

The stress distribution is not assumed on the opposite face, where force H2 acts. By analyzing the moment about the x-axis, force H2 is dependent on the depth below the top of the slab at which the resultant force acts, as seen in equation 3. Looking at equilibrium in the z-direction, H2 is dependent on the distance from the y-axis at which the resultant behaves, equation 4. This distance is denoted as variable a in Figure 4-7(a).

$$H2 = \frac{(LL + DL) * \left(\frac{L}{4}\right)}{Depth} \qquad (3)$$

$$H2 = \frac{H1 * (\frac{L}{4})}{a} \qquad (4)$$

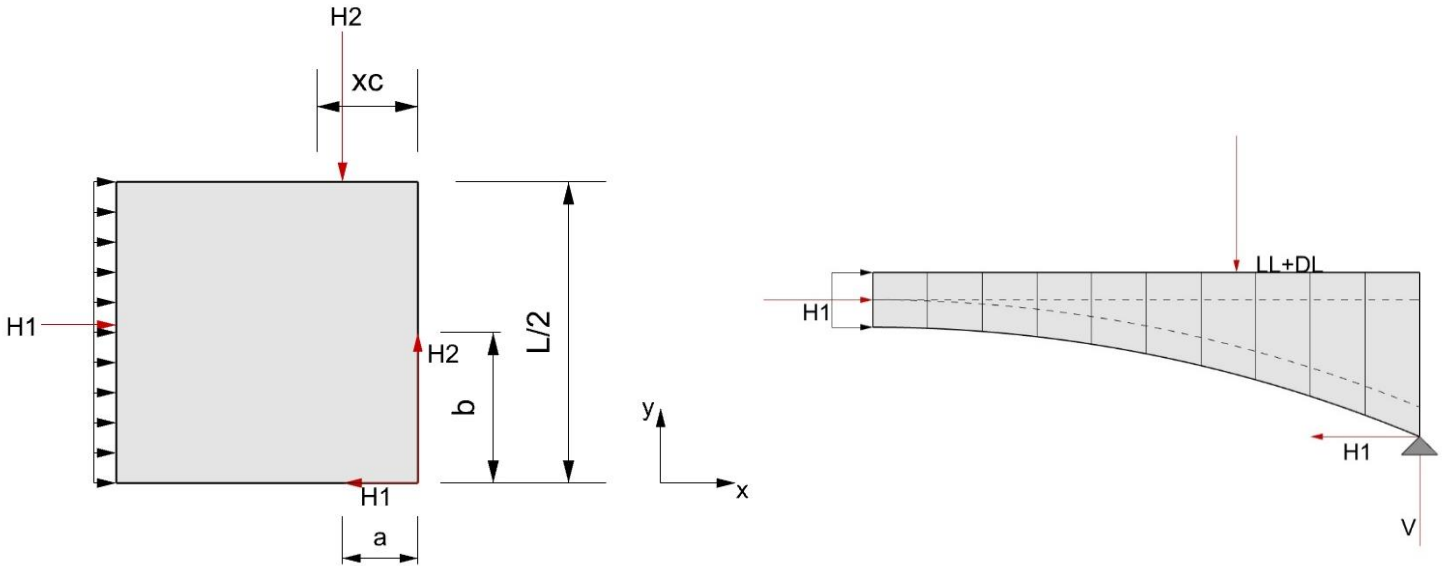

Figure 4-7: Plan view of offset forces (a) elevation view displaying support and direction of arch (b)

These two parameters, the distance from the y-axis and the depth of the resultant, are dependent on each other as seen in equation 5 below:

$$a = \frac{H1 * Depth}{LL + DL} \qquad (5)$$

where the depth variable represents the distance from the top at which the force acts. With the relationship displayed in equation 5, there is a maximum value that "a" could be while keeping the depth value within the set geometry of the system.

This rigid body assumption provides a minimum thrust value calculation to give an idea of the magnitude of thrust forces, and how the parameters of the stress distribution acting on the system effect these values.

4.2.2: Rigid Body Results

The rigid body stress assumption provides thrust values that are modestly lower than the 2D calculations. Figures 4-8 and 4-9 illustrates the decrease in thrust value for the two different fill densities in comparison to the results produced from the 2D calculations.

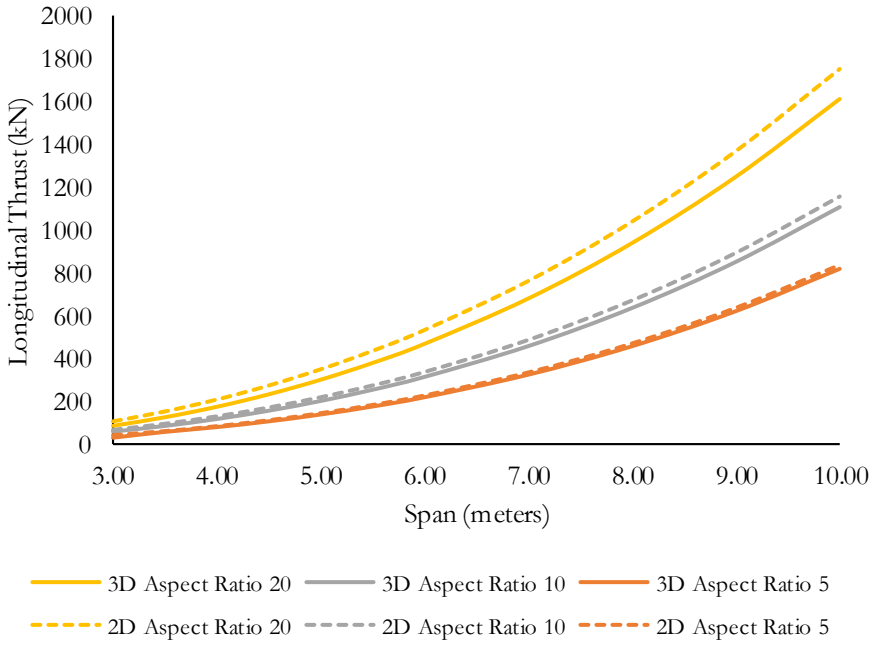

Figure 4-8: Rigid body thrust value comparison to 2D thrust results, fill density 2400 kg/m^3

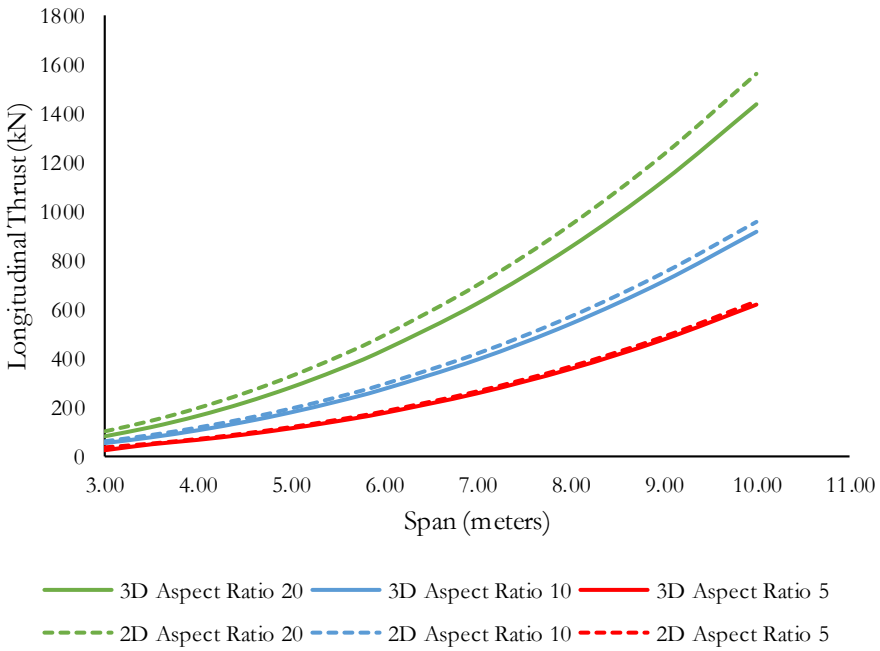

Figure 4-9: Rigid Body Thrust Value Comparison to 2D Thrust Results, Fill Density 1400 kg/m^3

For a fill density of 2400 kg/m^3 the thrust decreases from 2% to 28%, with the most significant reduction occurring at a span of 3 meters. By using a fill density of 1400 kg/m^3 the thrust decreases from 2% to 32%, with the most significant reduction occurring at the same span. However, the decrease in thrust comes at a cost, as there now exists thrust in the transverse direction that is not considered in the 2D calculations.

The methodology conducted in §4.2.1 to produce these results assumes that all of the force gets concentrated to the four corners of the system. In order to compute the stress acting at the corner, one must consider the resultant force of reactions H1, H2, and V, as seen in Figure 4-5, and the area over which that resultant force acts. Assuming that force behaves only over the area of one brick, as was assumed in all other calculations, would result in large, unrealistic stress results. It would be useful to further research the area over which the corner resultant force behaves through computational methods such as the force density method.

4.3: Three-Dimensional Analysis: Force Density Method

4.3.1: Background

The force density method is implemented in order to analyze the network of thrust lines within a given vault geometry. As mentioned in §2.3, the force density method is advantageous

because the equilibrium solution of any prescribed net of members can be found through linear algebra. This methodology assumes that the members, known as branches, within a network are connected to each other at nodes behaving as pinned joints, since shell structures have no flexural capacity. Each branch gets a specific force density assigned to it; altering the densities of each branch will result in a different shape as a result of the loads applied to the system, but all shapes will be in equilibrium. It should be noted, that a non-linear force density computation is possible, but not implemented in the scope of this thesis.

The process of using the force density method is well defined by Schek (1973). The methodology starts by defining a planar mesh of branches and nodes. The equilibrium solution of any net structure is dependent on which nodes are free to move and those that are constrained. The resulting shape of a network is defined by the branch node matrix, **C**, that describes the connection of a branch to the corresponding nodes that it connects. Each node has coordinates in the x, y, and z direction, denoted in vectors **x, y**, and **z,** from which a length and force vector of the branches, **L** and **s**, are defined. In this methodology, loads can only be applied to the nodes in the x, y, and z-direction defined by $\boldsymbol{P_x}$, $\boldsymbol{P_y}$, and $\boldsymbol{P_z}$. Two more sets of variables used in these calculations are the **u, v**, and **w** matrices representing the difference in coordinates between joined nodes as well as the **q** matrix defining the force densities. The matrix **Q** represents the diagonal of **q**. The equilibrium equations are used to simplify those seen in *equations 8-12*, where one solves for the free node coordinates **x, y,** and **z.** The matrix **D**, is used for organization. Lastly, it should be noted that the subscripts "f" seen in the equations represent the coordinates and loads acting on the fixed nodes.

$$D = C^T Q C \qquad (8)$$

$$D_f = C^T Q C_f \qquad (9)$$

$$x = D^{-1}(p_x - D_f x_f) \qquad (10)$$

$$y = D^{-1}(p_x - D_f y_f) \qquad (11)$$

$$z = D^{-1}(p_z - D_f z_f) \qquad (12)$$

Linkwitz (2014) provides an insightful chapter on using force densities to create a shape for a shell based on any network. The user defines the boundary conditions, organization of the mesh, force densities, and loads that will result in a specific shape in equilibrium. If the user is unsatisfied with the result then any of those four parameters can be altered to generate a new shape. The steps in this design process can be seen in Figure 4-10.

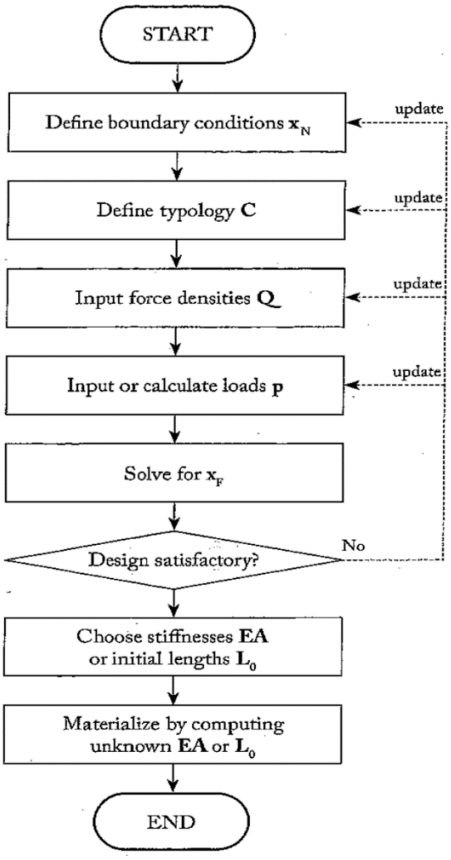

Figure 4-10: Flow chart for force density method (Linkwitz 2014)

This methodology set the procedure for the code that was implemented in Grasshopper and Rhino in order to generate compression only structures given different mesh sizes as well as loading scenarios. The force density procedure was coded in python, by Yijang Huang (Huang 2020), in which the user was required to input a mesh element, support nodes, force densities of the elements, and the loads applied. The script will assume that all the nodes that are not support nodes are free to move. The output of the python code is the resulting form found vault based upon set parameters. By adjusting the force densities or loads applied, users can observe the vault transform its shape in real time.

4.3.2: Force Density Configuration One Way Behavior

In order to ensure that equilibrium was being achieved, the original mesh was completely orthogonal, as can be seen in Figure 4-11, where the specified points along the two parallel edges represent the support points. The force densities are manipulated until the resulting thrust line

occurs at the midspan of the brick arch, in order to replicate the 2D calculations done in §3.2.1. If the system was in equilibrium, the total thrust should be the same as the results from the 2D analysis, just multiplied by the depth of the extrusion. It was confirmed that the total thrust calculated in Grasshopper perfectly matched the earlier hand calculations.

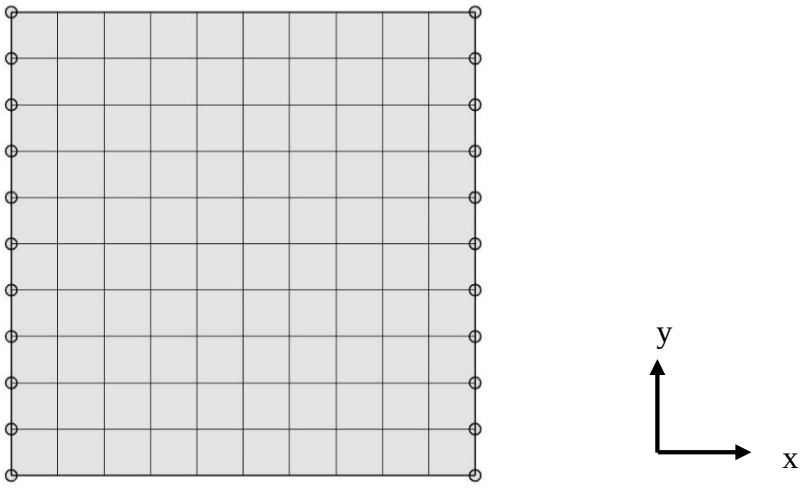

Figure 4-11: Initial orthogonal mesh

4.3.3: Force Density One Way Behavior Results

The vault in Figure 4.12(a), is the result of the initial orthogonal mesh for a 4x4 meter plan. The same loads were applied, as assumed in the 2D calculations seen in Figure 4-12(b). More load acts at the edges, as there is an increase in dead load from the fill towards the supports than at the crown. In order for the thrust line to lie within the middle half of the brick thickness, Figure 4-12(c), a force density of 71 and zero was applied to each member in the y and x direction, respectively.

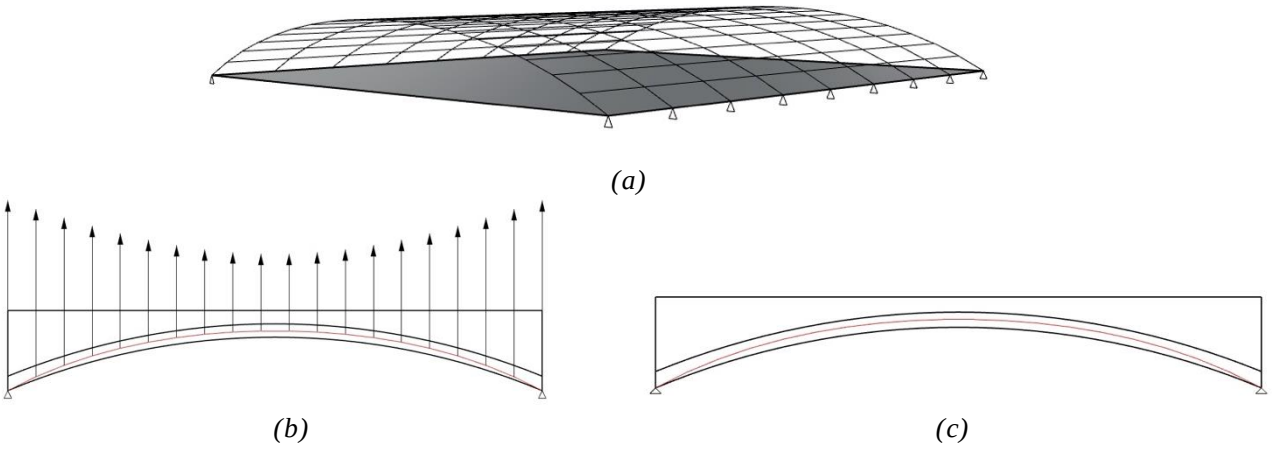

Figure 4-12: Generated thrust lines from FDM script (a) loading of the vaulted system (b) the thrust line (red line) acting within the vault (c)

order to achieve a vault with double curvature, the author implemented diagonals into the mesh configuration in the Python script, as discussed in §4.3.4.

4.3.4: Force Density Two Way Behavior

Since the FDM script is in equilibrium, more meshes including diagonal elements, could be used to explore possible equilibrium states. Specifically, the mesh in Figure 4-13 is used as it incorporates two-way behavior of the vaulted system. Adding diagonals to the system was only possible through the help of Demi Fang, who shared a grasshopper script that could easily change the coarseness of the mesh with the incorporation of diagonal members (Fang 2021). Ocne again, the vault remains supported at two parallel edges, denoted by the specified points.

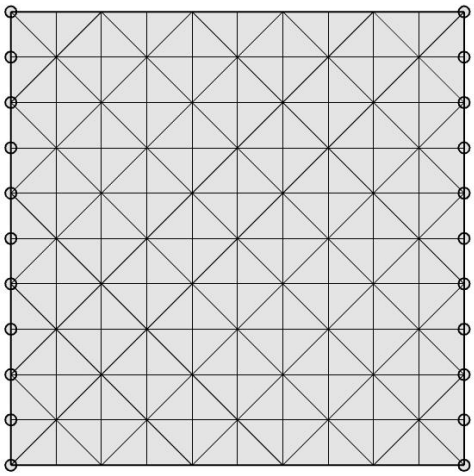

Figure 4-13: Diagonal mesh configuration, for force density method

4.3.5: Force Density Two Way Behavior Results

The configuration in Figure 4-13 has equal number of nodes as that of §4.3.2 and the same set of loads act on the new system. The resulting thrust configuration can be seen in Figure 4.14(a). With the new mesh as an input, double curvature exists for the vault, Figure 4-14(b), confirming 3D action. By manipulating the force densities, the thrust lines approximately behave within the thickness of the arch, as seen in Figure 4-14(c). The force density for each member is now 17.5, which is significantly lower than the force density value of §4.3.3, and the result is a 13% decrease in total thrust for the system compared to the purely 2D analysis.

For the orthogonal mesh configuration equivalent to 2D calculations, Figure 4-11, the total thrust acting on the system is 130 kN. By changing the mesh configuration to that of Figure 4-13 the total thrust acting on the system reduces to 113 kN or 13% lower.

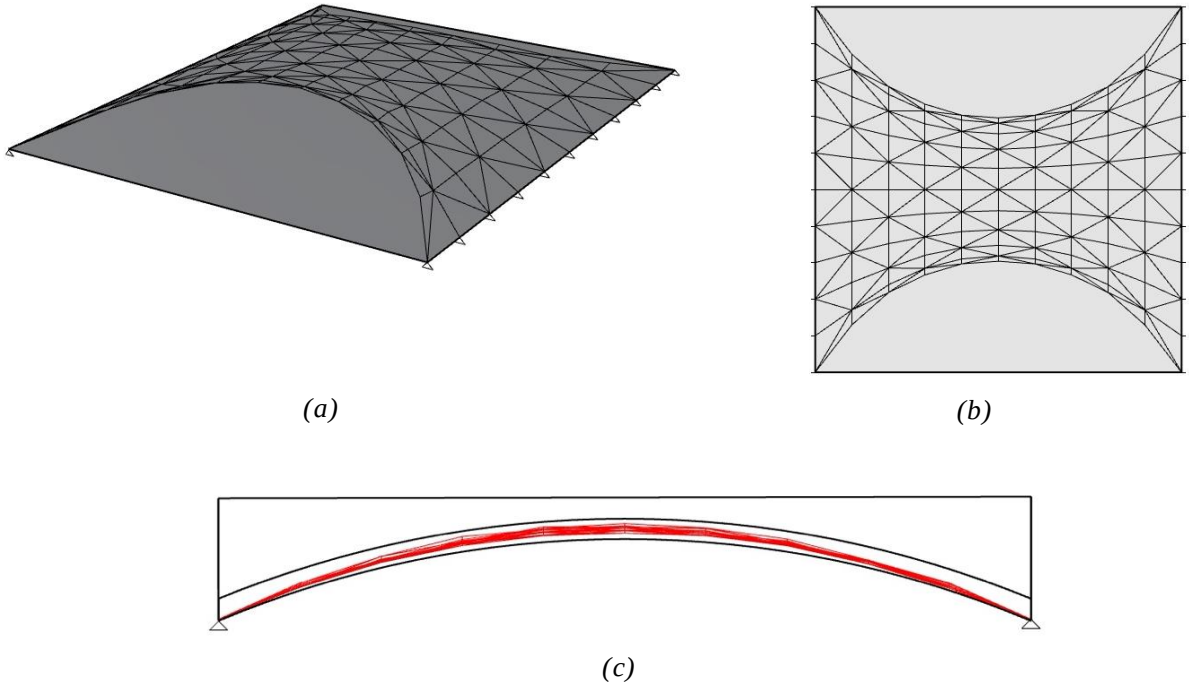

Figure 4-14: Force density solution for vault with diagonal mesh (a) axonometric view of solution (b) plan view displaying double curvature within the brick vault (c) section view

However, due to the boundary constraints, the resulting thrust configuration moves significantly inwards, and the loads move inwards with the nodes. While the same amount of vertical load is applied to the system as a whole, the loads no longer accurately represent the thrust lines for a vault loaded evenly but rather a vault with loads concentrated at the center. The front and back third of the system no longer have loads acting on them. The force density system

presented in this thesis is computationally intensive, and future research in determining how to incorporate loads to the front and back third sections is needed.

4.4 Chapter Summary

This chapter develops methodologies for analyzing the behavior of earthen vaulted floor systems in three dimensions. The idea of transverse behavior is first introduced in §4.1 assuming that not all forces travel directly to the midspan, but rather some force travels through the diagonals. This analysis revealed a small decrease in longitudinal thrust in comparison to the 2D calculations, but resulted in transverse thrust, and a decrease in flexure due to the vertical load. The rigid body configuration reduces the thrust more significantly and serves as a lower bound solution for the thrust acting on the vaulted system. The reduction in thrust decreases the amount of steel required. However, the area over which the force behaves is not as clearly defined, and the compressive stress acting on the brick in these regions remains a topic for future work. Lastly, the force density method analyzed the behavior of thrust lines within the vaulted system assuming different mesh configurations, resulting in a reduced thrust value for the entire system. Analyzing the behavior of forces within the vault in 3D leads to a decreased thrust value in comparison to the 2D analysis.

Out of all three proposed 3D analysis methods, the thesis recommends the use of the rigid body stress distribution, as it accurately portrays the loads acting on the system. This methodology, out of the three presented in this chapter, results in the largest decrease in thrust from the 2D calculations. The caveat with the rigid body stress distribution is that the area over which the force behaves is not as clear. It is recommended that future work investigates the actual stress distribution area to feasibly apply this method. Until then, the initial 2D results presented in Chapter 3 are sufficient and recommended to construct earthen vaulted floor systems.

Chapter 5 : Conclusion

5.1: Summary of Findings

This thesis set out to explore the range of geometries that vaulted earth floor systems can safely span in order to create sustainable, low-cost housing opportunities for developing economies. Through the use local materials, these structures will employ local labor, promoting the community's economy, while implementing the use of non-polluting material. Masonry vaults are currently being explored by organizations such as the Auroville Earth Institute, *Instituto de Bovedas Mexicanas, Association La Voute Nubienne,* and more, though there is much more research needed for earthen vaulted floor systems. Research began by talking to local builders in these organizations, giving greater perspective to the different techniques implemented in different parts of the world.

The analysis of masonry systems began by examining the atypical behavior of these structures, which cannot be analyzed through means of a standard fine element analysis, but rather must be evaluated through the use of limit analysis to compute the equilibrium of masonry arches. A two-dimensional analysis is conducted for a set of vaulted geometries considering different fill and brick materials. Having a baseline of selected results, allowed the research to progress forward with the analysis of the behavior of the barrel vault in three dimensions. For both 2D and 3D analysis, the masonry vaults were analyzed considering uniform dead and live loads for residential units.

Conclusions were drawn from the two-dimensional structural design analysis, assuming a uniform distribution of force acting only within the thickness of the brick arch (10 cm) itself and not the fill. As seen in Table 3-1, for a fill density of 2400 kg/m^3, and aspect ratio of 5 it is possible to span 3.75 m with adobe, 7.25 m with CEB, and 9.25 m with CSEB. For an aspect ratio of 10, it is possible to span 3.5 m with adobe, 7 m with CEB, and 9.25 m with CSEB. Lastly, for an aspect ratio of 20 it is no possible to span any appreciable length with adobe, but up to 5.5 m with CEB, and 7.5 m with CSEB.

Considering a lighter fill density of 1400 kg/m^3 and aspect ratio of 5 it is possible to span 4.5 m with adobe, 8.75 m with CEB, and 10 m with CSEB. For an aspect ratio of 10, it is possible to span 3.75 m with adobe, 8 m with CEB, and 10 m with CSEB. Lastly, for an aspect ratio of 20 it is not possible to span any appreciable length with adobe, but up to 5.75 m with CEB, and 8 m with CSEB.

For these sets of spans, the area of steel required to resists the tensile thrust exerted on the system is quantified in Appendix C below. Given the support conditions, extra steel may be necessary to withstand the flexural demand acting on the ring beam, which is quantified in Appendix D.

Analyzing the earthen vaulted floor systems in 3D yields smaller thrust values for all three methodologies explored in Chapter 4. Considering the rigid body stress distribution, the total thrust decreases by a maximum amount of 28% for a fill density of 2400 kg/m^3 and 32% for a fill density of 1400 kg/m^3. The force density methodology decreased the thrust as well, but only by 13%, suggesting the need for future work on the rigid body stress distribution. Given that the 2D calculations done in Chapter 3 are the clearest and easiest to replicate, the thesis recommends vaulted earthen floor systems be designed with this methodology.

5.2: Future Work

5.2.1: Continuation of 2D Analysis

There are a variety of ways in which the research on earthen vaulted floor systems can be progressed further. In regards to the 2D results, this thesis did not investigate lateral loads, which should be accounted for if the masonry vaults are to be built in seismic prone environments. Additionally, different stress distributions within the thickness of the vault could be analyzed and compared to the results produced in §3.3. Furthermore, investigating the structural capacity of the fill by allowing the thrust line to venture outside of the thickness of the arch is welcomed, as that would postulate a smaller thrust value and thus decrease the amount of steel necessary to support the vault. With this, asymmetrical live loading should be considered for the proposed system, including a collapse analysis. It would be useful to construct an experimental vault and load it to failure with an asymmetrical applied load as a validation for the methods presented in this thesis.

5.2.3 Continuation of 3D Analysis

In regards to the 3D methodology, §4.2 analyzes a stress distribution behaving on a rigid body in order to calculate the total thrust exerted by the system, assuming the vault is supported on the corners. Given that the forces concur to the corners, the area over which the force acts are not as clear. Assuming that the force behaves only over the area of one brick results in stress

values that are three times as high as those observed in Figures 3.5-6. Using computational methods such as the Airy stress function or dynamic relaxation could be used to estimate the true area over which the force acts at the corner.

Additionally, the force density method can be further researched, by creating a model that does not move the location of the loads towards the middle third of the span. The calculations done in §4.3, resulted in a decrease in thrust of approximately 13% with the caveat that significantly more loads behave in the middle third of the vault than the realistic behavior. With this, no load behaves in the front and back end of the vault. It is suggested that the force density method is coded such that each node is fixed in the x and y directions and only the z variable is allowed to vary. With this correction, the system should be reanalyzed with the force density methodology or with other 3D equilibrium methods such as thrust network analysis.

Bibliography

Adiels, Emil, Mats Ander, and Chris Williams. 2017. "Brick Patterns on Shells Using Geodesic Coordinates."

Adriaenssens, Sigrid, Philippe Block, Diederik Veenendaal, and Chris Williams, eds. 2014. *Shell Structures for Architecture: Form Finding and Optimization*. London ; New York: Routledge/ Taylor & Francis Group.

Aguirre, Ramon. 2021. Personal Communication with author.

Allen, Edward, and Waclaw Zalewski. 2012. *Form and Forces Designing Efficient, Expressive Structures*. https://nbn-resolving.org/urn:nbn:de:101:1-201412189237.

ASCE 2011 Publications. 2010. ASCE Press Series. American Society of Civil Engineers. https://books.google.com/books?id=PAv_wAEACAAJ.

"AVD Construction." 2021. Auroville Earth Institute. Accessed January 15, 2021. http://www.earth-auroville.com/avd_construction_en.php

Barentin, Cristián Calvo, Ioannis-Athanasios Zornatzis, Gnanli Landrou, Thibault Demoulin, Guillaume Habert, and Philippe Block. 2020. "When Low Strength Materials Meet Funicular Structures: A Sustainable Clay Floor Structure Solution for Emerging Contexts." *IOP Conference Series: Earth and Environmental Science* 588 (November): 042024. https://doi.org/10.1088/1755-1315/588/4/042024.

Beall, Christine. 2012. *Masonry Design and Detailing*. 6th ed. New York: McGraw-Hill.

"Brick Masonry Arches." 1995. Technical Notes 31. The Brick Industry Association.

Block, Philippe, Thierry Ciblac, and John Ochsendorf. 2006. "Real-Time Limit Analysis of Vaulted Masonry Buildings." *Computers & Structures* 84 (29): 1841–52. https://doi.org/10.1016/j.compstruc.2006.08.002.

Block, Philippe, Matt DeJong, and John Ochsendorf. 2006. "As Hangs the Flexible Line: Equilibrium of Masonry Arches." *Nexus Network Journal* 8 (2): 13–24. https://doi.org/10.1007/s00004-006-0015-9.

Block, P., and Lorenz Lachauer. 2011. "Closest-Fit, Compression-Only Solutions for Freeform Shells."

"Compressed Stabilized Earth Block."2020. Auroville Earth Institute. Accessed January 15, 2021. http://www.earth-auroville.com/compressed_stabilised_earth_block_en.php.

"COVID-19 in Slums and Social Housing in Central American and the Dominic Republic," 2021. Eurosocial. Accessed April 19, 2020. https://eurosocial.eu/en/actualidad/covid-19-in-slums-and-social-housing-in-central-america-and-the-dominican-republic/.

Dahmen, J. F. D., and J. A. Ochsendorfs. 2012. "17 - Earth Masonry Structures: Arches, Vaults and Domes." In *Modern Earth Buildings*, edited by Matthew R. Hall, Rick Lindsay, and Meror Krayenhoff, 427–60. Woodhead Publishing Series in Energy. Woodhead Publishing. https://doi.org/10.1533/9780857096166.4.427.

Davis, Lara. 2021. Personal Communication with author.

El-Derby, Abdou, and Ahmed Elyamani. 2016. "The Adobe Barrel Vaulted Structures in Ancient Egypt: A Study of Two Case Studies for Conservation Purposes." *Mediterranean Archaeology and Archaeometry* 16: 295–315. https://doi.org/10.5281/zenodo.46361.

Fang, Demi. 2020. *Topologies Grasshopper Script*.

"Goal 11: Make Cities Inclusive, Sage, Resilient and Sustainable." 2020. United Nations. Accessed April 11, 2021.

Hebel, Dirk, Melakeselam Moges, Zara Gray, Eidgenössische Technische Hochschule Zürich, Ethiopian Institute of Architecture, Building Construction and City Development, and Something Fantastic, eds. 2015. *SUDU. 2: Manual*. Berlin: Ruby Press.

Heyman, Jacques and Cambridge Core. 1997. *The Stone Skeleton: Structural Engineering of Masonry Architecture*. Cambridge: Cambridge University Press.

Huang, Yijang. 2020. *Force Density Method Python Script*.

Illampas, Rogiros, Ioannis Ioannou, and Dimos Charmpis. 2011. "A Study of the Mechanical Behaviour of Adobe Masonry." In *WIT Transactions on the Built Environment*, 118:485–96. https://doi.org/10.2495/STR110401.

Indian Standard IS 6332 (1984). *Code of practice for construction of floors and roofs using precast doubly-curved shell units*. Indian Standards Institution: New Delhi

International Code Council. 2009. *IBC: International Building Code*. Country Club Hills, IL: International Code Council.

"Introduction to Vaulted Structures." 2021. Auroville Earth Institute. Accessed January 21, 2021. http://www.earth-auroville.com/vaulted_structures_introduction_en.php

Jagoe, Grace. 2021. "Autoclaved Aerated Concrete Tile Vaults for Lightweight Floor Systems." Massachusetts Institute of Technology.

López, David, T. Mele, and P. Block. 2016. "Tile Vaulting in the 21st Century." *Informes de La Construcción* 68: 162. https://doi.org/10.3989/ic.15.169.m15.

Maini, S and Davis, L. 2020. *Building with Arches, Vaults and Domes: Training Manual for Architects and Engineers*. Auroville Earth Institute, ref. TM 04.

Newman, Alexander. 2021. *Structural Renovation of Buildings: Methods, Details, and Design Examples*. Second edition. New York: McGraw Hill.

New Mexico Administrative Code. 2015. "2015 New Mexico Earthen Building Materials Code." 14.7.4 NMAC.

"Nosotros." 2021. IBOMEX. Accessed April 20, 2021.

Oates, David. 1990. "Innovations in Mud-brick: Decorative and Structural Techniques in Ancient Mesopotamia." *World Archaeology* 21 (3): 388–406. https://doi.org/10.1080/00438243.1990.9980115.

Ramage, Michael H., John Ochsendorf, and Peter Rich. 2010. "Sustainable Shells: New African Vaults Built with Soil-Cement Tiles" 51 (4): 255–61.

Schek, H.-J. 1974. "The Force Density Method for Form Finding and Computation of General Networks." *Computer Methods in Applied Mechanics and Engineering* 3 (1): 115–34. https://doi.org/10.1016/0045-7825(74)90045-0.

Seattle Department of Construction & Inspection. 2015. "Section 2107 Allowable Stress Design." In *2015 Seattle Building Code*, 517. http://www.seattle.gov/documents/Departments/SDCI/Codes/SeattleBuildingCode/2015SBCChapter21.pdf

Steele, James, and Hassan Fathy. 1988. *Hassan Fathy*. Architectural Monographs 13. London: Acad. Ed. [u.a.].

"The Program." 2021. La Voute Nubienne. Accessed April 5, 2021.

Triveno, Luis, and Olivia Nielsen. n.d. "It's Time to Start Solving Latin America's Migration Cris with Creative Housing Solutions." *World Bank Blogs* (blog). https://blogs.worldbank.org/sustainablecities/its-time-start-solving-latin-americas-migration-crisis-creative-housing-solutions.

"Urbanization in Latin America." 2017. BBVA Research.

Veenendaal, D., and P. Block. 2012. "An Overview and Comparison of Structural Form Finding Methods for General Networks." *International Journal of Solids and Structures* 49 (26): 3741–53. https://doi.org/10.1016/j.ijsolstr.2012.08.008.

Wilson, Samuel H. 2016. “Structural Design of Shallow Masonry Domes.” Massachusetts Institute of Technology.

Appendix A: Sample Calculation for Determining Thrust of System

This guide is intended to show builders the calculations done in order to estimate the amount of thrust exerted by a system, so that they may be replicated for different materials and geometries. The calculations are based on a uniform stress distribution acting along the thickness of the brick as discusses in §3.2.

Parameters:

- Span (L): 4 meters
- Rise (R): 0.4 meters
- Depth into the page (D): 1 meter
- Section Width (S): .2 meters
- Section Height (H): changes per section
- 5X10X20 cm brick, used for vault and slab
    - Weight (W): 1900 (N/m^2)
- Earthen Fill
    - Density (ρ): 2400 kg/m^3
- Live Load
    - LL: 1900 (N/m^2)

Step 1: Split half the arch into ten equal segments, calculate the centroid of each segment, depicted by the red circles below:

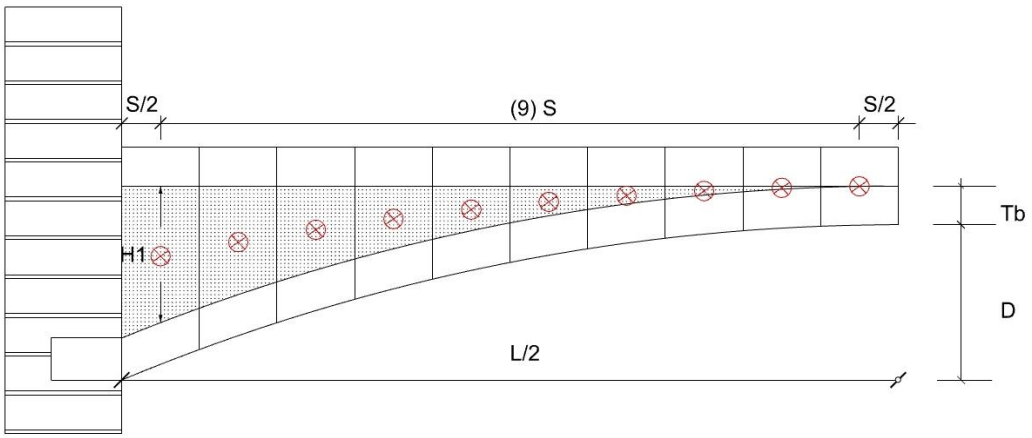

Step 2: Calculate the dead load due to the fill, slab, and brick acting at each segment through the following formula:

$$DL_{fill} = S * H_i * \rho * g * D$$

$$DL_{slab} = S * W * D$$

$$DL_{brick\ arch} = S * W * D$$

Where g represents gravity.

Step 3: Calculate the resultant from the uniform live load acting on the system:

$$LL = LL * W * L/2$$

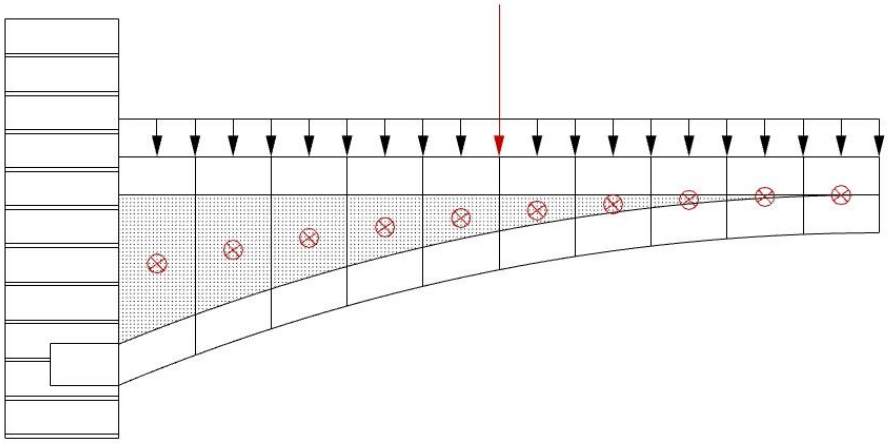

Step 4: All the forces on acting on half of the vault now look as such:

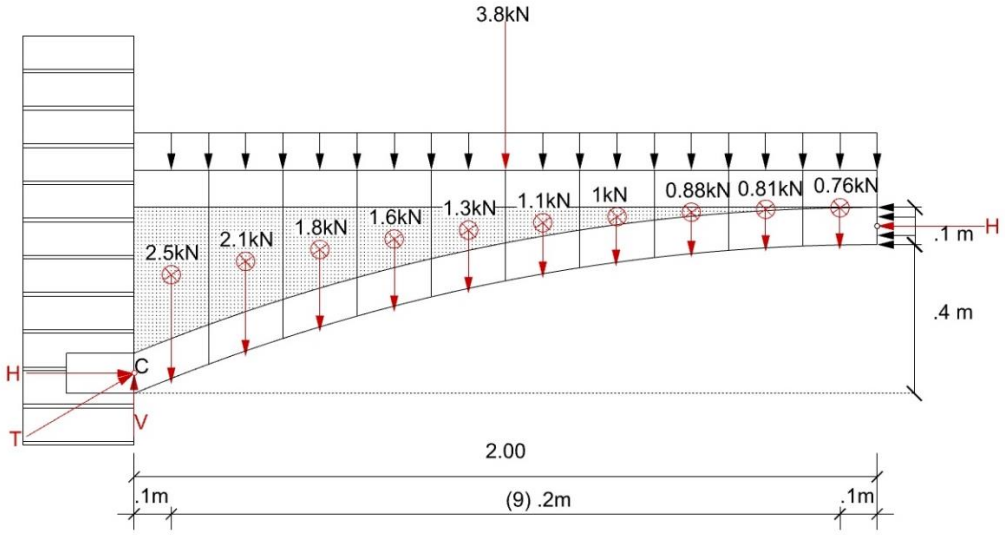

Step 5: Take moments about Point C, with respective to each forces moment arm to obtain the thrust value, H:

$$\sum M_c = (2.5kN * .1m) + (2.1kN * .3m) + (1.8kN * .5m) + (1.6kN * .7m) + (1.3kN * .9m) + (1.1kN * 1.1m) + (1kN * 1.3m) + (.88kN * 1.5) + (.81kN * 1.7) * (.76 * 1.9) + (3.8kN * 1m) - (H * .4m) = 0$$

By solving for H, one obtains 32.4 kN for a one-meter strip. For the entire 4X4 vault the total thrust is 129.8 kN.

Appendix B: Fill Density Calculations

The following calculations were produced by Carene T. Umubyeyi to estimate the change in fill density for a glass bottle configuration, as mentioned in §3.2.2. The calculations are based on the analysis of a 25x25 cm area with a 1-meter depth, as seen below:

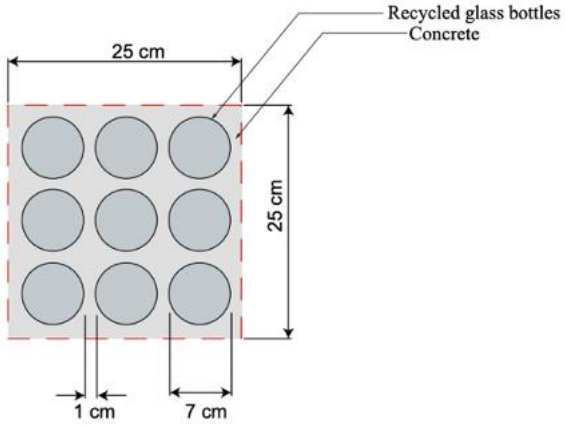

$Concrete\ Volume = 100\ cm * (625\, cm^2) - 9 * (38.5 cm^2)(100 cm) = 27850\ cm^3$

$Glass\ Volume = 100\ cm * (7.6\ cm^2) * 9 + 9 * (19.2 cm^3)(2) = 7186\ cm^3$

$\rho_{concrete} = 2.4 \frac{g}{cm^3}$

$\rho_{glass} = 2.9 \frac{g}{cm^3}$

$Weight\ of\ 25cm\ by\ 25cm\ block$: $27850\ cm^3 \left(2.4 \frac{g}{cm^3}\right) + 7186\ cm^3 \left(2.9 \frac{g}{cm^3}\right) = 87.7\ kg$

$Weight\ of\ 1m\ by\ 1m\ by\ 1m\ block = 16 * (87.7 kg) = 1403\ kg$

$Density\ of\ concrete\ fill\ with\ glass\ bottles$: $\mathbf{1400\ kg/m^3\ \ compared to\ 2400\ kg/m^3}$

Appendix C: Design Guide Quantifying Tensile Steel Requirement

The following design charts are created using an admissible stress for steel of 250 MPa. As a factor of safety, this value was taken to be 125 MPa, which is approximately 1,250 kg/cm^2. The horizontal thrust values are computed from two-dimension analysis presented in Chapter 3. The following steel quantities are tabulated to resist tensile demand ONLY. Flexural demand is considered in Appendix D.

Case 1 Parameters

- Density of Fill = 2400 kg/m^3
- $F_y = 1250\,\frac{kg}{cm^2} = 12.3\,\frac{kN}{cm^2}$

Furthering the sample calculation done in Appendix A the area of steel required was calculated as such for a 4X4 meter area with a rise of .4 meters:

$$\frac{Total\ Thrust}{Fy} = \frac{129.8\,kN}{12.3\,\frac{kN}{cm^2}} = 10.6cm^2$$

Aspect Ratio 5					
Span (m)	Rise (m)	Aspect Ratio	Thrust (kN)	Area of Steel Required cm^2	Volume cm^3
3.0	0.60	5.0	42.1	3.43	1029.5
3.5	0.70	5.0	60.8	4.96	1734.7
4.0	0.80	5.0	90.7	7.40	2959.3
4.5	0.90	5.0	119.3	9.73	4379.7
5.0	1.00	5.0	144.5	11.8	5890.2
5.5	1.10	5.0	192.3	15.7	8623.8
6.0	1.20	5.0	227.0	18.5	11106.7
7.0	1.40	5.0	334.4	27.3	19091.3
8.0	1.60	5.0	469.8	38.3	30649.4
9.0	1.80	5.0	636.1	51.9	46684.4

Aspect Ratio 10					
Span	Rise	Aspect Ratio	Thrust	Area of Steel Required cm^2	Volume cm^3
3.0	0.30	10.0	66.6	5.43	1628.3
3.5	0.35	10.0	95.2	7.76	2716.2
4.0	0.40	10.0	129.8	10.6	4235.1
4.5	0.45	10.0	170.9	13.9	6272.9
5.0	0.50	10.0	218.9	17.8	8923.8
5.5	0.55	10.0	274.0	22.3	12288.1
6.0	0.60	10.0	336.6	27.5	16472.1
7.0	0.70	10.0	486.2	39.7	27755.5
8.0	0.80	10.0	670.6	54.7	43747.6
9.0	0.90	10.0	892.7	72.8	65520.1

Aspect Ratio 20					
Span	Rise	Aspect Ratio	Thrust	Area of Steel Required cm^2	Volume cm^3
3.0	0.15	20.0	106.3	8.67	2601.4
3.5	0.18	20.0	152.5	12.4	4352.0
4.0	0.20	20.0	208.0	17.0	6786.5
4.5	0.23	20.0	273.4	22.3	10034.7
5.0	0.25	20.0	349.1	28.5	14232.7
5.5	0.28	20.0	435.3	35.5	19522.6
6.0	0.30	20.0	532.5	43.4	26053.0
7.0	0.35	20.0	761.3	62.1	43459.2
8.0	0.40	20.0	1038.6	84.7	67760.9
9.0	0.45	20.0	1367.5	111.5	100366.1

Case 2:

- Density of Fill = 1400 kg/m^3
- $F_y = 1250\,\frac{kg}{cm^2} = 12.3\,\frac{kN}{cm^2}$

Aspect Ratio 5					
Span (m)	Rise (m)	Aspect Ratio	Thrust (kN)	Area of Steel Required cm^2	Volume cm^3
3.0	0.60	5.0	36.9	3.01	902.4
3.5	0.70	5.0	52.4	4.28	1496.6
4.0	0.80	5.0	71.3	5.81	2324.6
4.5	0.90	5.0	93.6	7.63	3434.6
5.0	1.00	5.0	119.6	9.76	4878.3
5.5	1.10	5.0	149.6	12.2	6711.0
6.0	1.20	5.0	183.8	15.0	8991.7
7.0	1.40	5.0	265.4	21.6	15150.4
8.0	1.60	5.0	366.3	29.9	23897.2
9.0	1.80	5.0	488.2	39.8	35832.2
10.0	2.00	5.0	632.9	51.6	51612.7

Aspect Ratio 10					
Span (m)	Rise (m)	Aspect Ratio	Thrust (kN)	Area of Steel Required cm^2	Volume cm^3
3.0	0.30	10.0	61.7	5.03	1510.3
3.5	0.35	10.0	87.3	7.12	2493.0
4.0	0.40	10.0	118.0	9.62	3848.2
4.5	0.45	10.0	153.8	12.5	5645.5
5.0	0.50	10.0	195.2	15.9	7957.9
5.5	0.55	10.0	242.2	19.7	10862.1
6.0	0.60	10.0	295.1	24.1	14438.4
7.0	0.70	10.0	419.5	34.2	23945.9
8.0	0.80	10.0	570.1	46.5	37194.0
9.0	0.90	10.0	748.7	61.1	54953.5
10.0	1.00	10.0	957.1	78.1	78052.4

Aspect Ratio 20					
Span (m)	Rise (m)	Aspect Ratio	Thrust (kN)	Area of Steel Required cm^2	Volume cm^3
3.0	0.15	20.0	102.1	8.33	2498.1
3.5	0.18	20.0	145.5	11.9	4153.6
4.0	0.20	20.0	197.4	16.1	6438.3
4.5	0.23	20.0	257.9	21.0	9464.3
5.0	0.25	20.0	327.3	26.7	13347.2
5.5	0.28	20.0	405.9	33.1	18206.4
6.0	0.30	20.0	493.9	40.3	24164.6
7.0	0.35	20.0	698.7	57.0	39887.7
8.0	0.40	20.0	943.8	77.0	61571.4
9.0	0.45	20.0	1230.7	100.4	90327.8
10.0	0.50	20.0	1561.3	127.3	127326.3

Appendix D: Design Guide Quantifying Flexural Steel Requirement

The following design charts are created, with the help of Carene T. Umubyeyi, using an admissible stress for steel of 250 MPa. As a factor of safety, this value was taken to be 125 MPa, which is approximately 1,250 $\frac{kg}{cm^2}$. The following steel quantities are tabulated to resist flexural demand ONLY in the case that the vault is not constructed on a support wall.

Case 1 Parameters:

- Density of Fill = 2400 kg/m^3
- $F_y = 1250\,\frac{kg}{cm^2} = 12.3\,\frac{kN}{cm^2}$

Aspect Ratio 5					
Span (m)	Rise (m)	Aspect Ratio	Vertical Force (kN) every meter	Area of Steel Required cm^2	Volume cm^3
3.0	0.60	5.0	15.7	12.9	3870.0
3.5	0.70	5.0	19.6	19.4	6772.5
4.0	0.80	5.0	24.0	25.8	10320.0
4.5	0.90	5.0	28.8	32.8	14742.0
5.0	1.00	5.0	34.0	38.7	19350.0
5.5	1.10	5.0	39.6	50.3	27665.0
6.0	1.20	5.0	45.5	65.5	39312.0
7.0	1.40	5.0	58.6	98.3	68796.0
8.0	1.60	5.0	73.3	130.7	104544.0
9.0	1.80	5.0	89.6	180.7	162603.0
10.0	2.0	5.0	107.5	206.5	206480.0

Aspect Ratio 10					
Span	Rise	Aspect Ratio	Vertical Force (kN) every meter	Area of Steel Required cm^2	Volume cm^3
3.0	0.30	10.0	12.1	11.6	3483.0
3.5	0.35	10.0	14.8	15.3	5344.5
4.0	0.40	10.0	17.7	20.4	8144.0
4.5	0.45	10.0	20.8	25.8	11610.0
5.0	0.50	10.0	24.1	32.8	16380.0
5.5	0.55	10.0	27.6	38.7	21285.0
6.0	0.60	10.0	31.3	49.1	29484.0
7.0	0.70	10.0	39.3	72.6	50820.0
8.0	0.80	10.0	48.1	90.5	72432.0
9.0	0.90	10.0	57.6	129.1	116145.0
10.0	1.0	10.0	68.0	154.9	154860.0

Aspect Ratio 20					
Span	Rise	Aspect Ratio	Vertical Force (kN) every meter	Area of Steel Required cm^2	Volume cm^3
3.0	0.15	20.0	10.3	10.2	3054.0
3.5	0.18	20.0	12.4	15.3	5344.5
4.0	0.20	20.0	14.6	19.4	7740.0
4.5	0.23	20.0	16.8	24.6	11056.5
5.0	0.25	20.0	19.2	30.2	15090.0
5.5	0.28	20.0	21.6	38.7	21285.0
6.0	0.30	20.0	24.2	45.2	27090.0
7.0	0.35	20.0	29.6	60.4	42252.0
8.0	0.40	20.0	35.4	80.5	64384.0
9.0	0.45	20.0	41.6	103.2	92916.0
10.0	0.50	20.0	48.2	129.1	129050.0

Case 2:

- Density of Fill = 1400 kg/m^3
- $F_y = 1250\ \frac{kg}{cm^2} = 12.3\ \frac{kN}{cm^2}$

Aspect Ratio 5					
Span (m)	Rise (m)	Aspect Ratio	Vertical Force (kN) every meter	Area of Steel Required cm^2	Volume cm^3
3.0	0.60	5.0	12.7	11.6	3483.0
3.5	0.70	5.0	15.6	15.3	5344.5
4.0	0.80	5.0	18.8	20.1	8048.0
4.5	0.90	5.0	22.2	29.0	13068.0
5.0	1.00	5.0	25.8	35.6	17815.0
5.5	1.10	5.0	29.6	41.0	22522.5
6.0	1.20	5.0	33.7	50.3	30180.0
7.0	1.40	5.0	42.5	72.6	50820.0
8.0	1.60	5.0	52.3	103.2	82592.0
9.0	1.80	5.0	63.0	129.1	116145.0
10.0	2.00	5.0	74.6	180.7	180670.0

Aspect Ratio 10					
Span (m)	Rise (m)	Aspect Ratio	Vertical Force (kN) every meter	Area of Steel Required cm^2	Volume cm^3
3.0	0.30	10.0	10.6	11.4	3408.0
3.5	0.35	10.0	12.8	12.9	4515.0
4.0	0.40	10.0	15.1	16.4	6552.0
4.5	0.45	10.0	17.5	24.6	11056.5
5.0	0.50	10.0	20.0	29.0	14520.0
5.5	0.55	10.0	22.6	38.7	21285.0
6.0	0.60	10.0	25.4	43.6	26136.0
7.0	0.70	10.0	31.2	60.4	42252.0
8.0	0.80	10.0	37.6	77.4	61944.0
9.0	0.90	10.0	44.3	103.2	92916.0
10.0	1.00	10.0	51.6	154.9	154860.0

Aspect Ratio 20					
Span (m)	Rise (m)	Aspect Ratio	Vertical Force (kN) every meter	Area of Steel Required cm^2	Volume cm^3
3.0	0.15	20.0	9.6	10.0	3000.0
3.5	0.18	20.0	11.4	11.6	4063.5
4.0	0.20	20.0	13.2	15.3	6108.0
4.5	0.23	20.0	15.2	20.1	9054.0
5.0	0.25	20.0	17.1	29.0	14520.0
5.5	0.28	20.0	19.2	32.8	18018.0
6.0	0.30	20.0	21.2	38.7	23220.0
7.0	0.35	20.0	25.6	50.3	35210.0
8.0	0.40	20.0	30.2	72.6	58080.0
9.0	0.45	20.0	35.0	87.1	78408.0
10.0	0.50	20.0	40.0	129.1	129050.0